

Chapter 8

Long-Term Analysis of Water Quality in Chilika Lagoon and Application of Bio-optical Models for Cyclone Impact Assessment



Abhishek Kumar, Sk. Md. Equeenuddin, and Deepak R. Mishra

Abstract A comprehensive analysis of sediment and phytoplankton dynamics in Chilika lagoon by synthesizing various remote sensing datasets is presented in this study. The goal of the study was to monitor and analyze the spatio-temporal variability of total suspended sediment (TSS) and chlorophyll-a (chl-a) concentration and associated environmental forcings in the coastal lagoon. NASA's Moderate Resolution Imaging Spectroradiometer (MODIS) surface reflectance cloud free data was used to develop a TSS and chl-a model. Finally, a case study showing implication of satellite based TSS and Chl-*a* models to assess the impacts of natural hazards such as cyclones on water quality of Chilika Lagoon is presented. This case study is based on comparing the effect of two anniversary very severe cyclonic storms (VSCSs): category-5 Phailin (12 October, 2013) and category-4 Hudhud (12 October, 2014) that impacted the lagoon. Analysis for 14 years (2001–2014) using MODIS 8-day composites (MOD09Q1) data indicated that the seasonal variability of TSS is dominant in all the three sectors of the lagoon compared to inter-annual variability. The main reason for large variations in the northern sector is the shallow depth and intrusion of large sediment discharge from Mahanadi River from the northern side, which is the largest fresh water distributary for Chilika Lagoon. Anniversary cyclone impact analysis revealed that *Phailin's* impact on Chilika Lagoon and its watershed resulted in unprecedented levels of precipitation and runoff before-during-after the landfall, which shattered the typical sectorial turbidity gradient. Exponential increase in turbidity because of a combination of run-off and wind driven re-suspension of fine sediments resulted in strong attenuation of light in water column post-*Phailin*. Limited light condition coupled with

A. Kumar · D. R. Mishra (✉)

Center for Geospatial Research, Department of Geography, University of Georgia, Athens, GA, USA

e-mail: dmishra@uga.edu

S. M. Equeenuddin

Department of Earth & Atmospheric Sciences, National Institute of Technology, Rourkela, Odisha, India

© Springer Nature Switzerland AG 2020

C. M. Finlayson et al. (eds.), *Ecology, Conservation, and Restoration of Chilika Lagoon, India*, Wetlands: Ecology, Conservation and Management 6,

https://doi.org/10.1007/978-3-030-33424-6_8

165

enhanced flushing rate due to flooded river and increased freshwater discharge reduced the Chl-*a* concentration after the passage of *Phailin*. In contrast, relatively farther landfall location, trajectory away from the lagoon, relatively lower wind intensity and short duration of stay of VSCS *Hudhud*, led to lesser precipitation and surface runoff compared to *Phailin*. Consequently, lagoon did not experience a drastic increase in turbidity and light attenuation. Sufficient light availability, stable wind, reduced flushing all favored the phytoplankton growth after passage of *Hudhud* and thus, Chl-*a* concentration increased almost threefold in all the sectors of the lagoon. The approach used in this study can be applied to other cyclone-prone coastal areas. Coupling of satellite based observation with modelling output from systems such as Giovanni can improve monitoring program implemented in numerous coastal estuaries and lagoons.

Keywords Phailin · Hudhud · MODIS · Giovanni · Chilika Lagoon · Suspended sediment · Chlorophyll-*a* · Algal bloom

8.1 Introduction

Coastal lagoons are among one of the most productive, complex, and dynamic ecosystems around the world as they are positioned at the interface of rivers and sea (Mishra et al. 2017; Srichandan et al. 2015). India has such a productive and complex lagoon named “Chilika” which is Asia’s largest and world’s second largest brackish water lagoon situated in Odisha state along the east coast at latitude 19°28′ – 19°54′ north, longitude 85°06′ – 85°35′ east. The lagoon has a spread of about 64 km in length from northeast to southwest along the Odisha coast and connected to the Bay of Bengal (BOB) (Fig. 8.1a). Based on salinity and depth, the lagoon is conventionally subdivided into four sub-regions (CDA 2008), namely northern sector (NS), central sector (CS), southern sector (SS) and outer channel (OC) (Fig. 8.1a). It receives fresh water mainly from three distributaries of Mahanadi River namely Nuna, Daya, and Bhargavi as shown in Fig. 8.1a.

Chilika is a shallow coastal lagoon with average depth of 1.8 m and exhibits variability in water coverage area from 1165 to 906 km² during monsoon and summer respectively (Siddiqi and Rama Rao 1995). Apart from being shallow and productive, Chilika is well known for its unique assemblages of fresh, brackish, and marine water ecosystem with estuarine character and supports more than 200,000 fishermen in the surrounding 132 villages (CDA 2008). Because of its rich biodiversity and socio-ecological values, the lagoon is designated as “Ramsar Site” a wetland of international importance (Srichandan et al. 2015). However, water quality of the lagoon has been degrading over the years due to factors such as siltation, change in salinity, increase in fresh water weeds, and eutrophication (Nayak et al. 2004; Jayaraman et al. 2005; Bramha et al. 2008; Panda and Mohanty 2008; Panigrahi et al. 2009). One of the main problems the lagoon is facing among all of the above is the decrease in overall salinity due to narrowing of the lagoon’s mouth

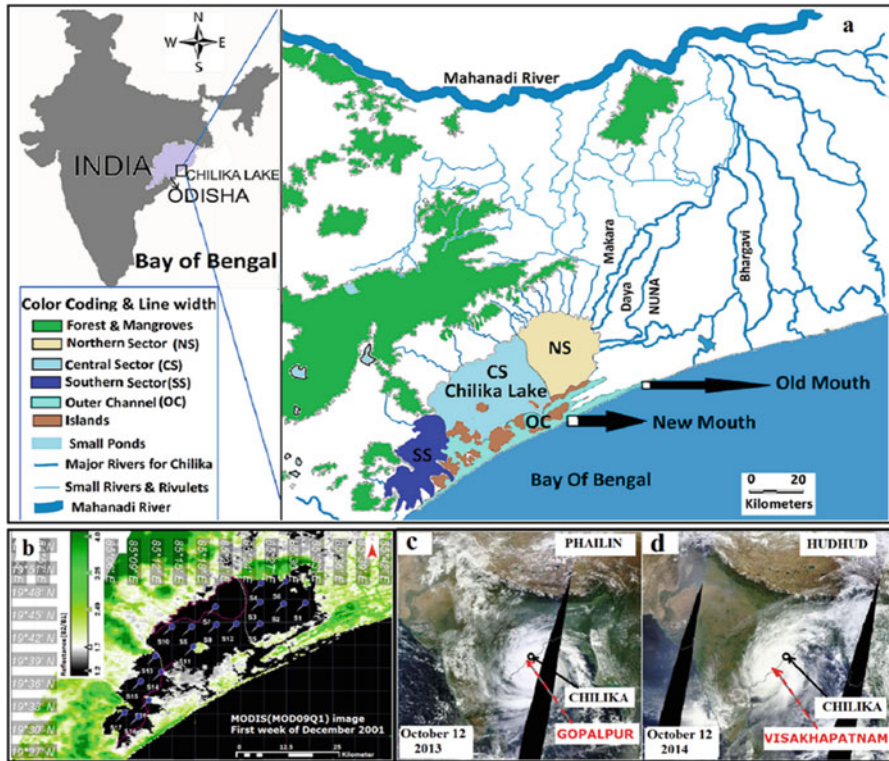


Fig. 8.1 Map of Chilika Lagoon showing the sub-regions of the lagoon and major tributaries (Daya, Nuna, Bhargavi, and Makara) of Mahanadi River (Largest fresh water source for lagoon) (a). The sub-regions are northern sector (NS), central sector (CS), southern sector (SS) and outer channel (OC). MODIS image (MOD09Q1) with sampling locations used for long-term quantitative analysis of TSS in different sectors of the lagoon (b). The forest cover and emergent vegetation in the west and upper part of northern side is shown in green, water area in black, and land area in white/gray (b). Areas which are typically covered by submerged vegetation and weeds are indicated by red line polygon (b). It should be noted that the sampling locations used in long-term TSS analysis were devoid of interference from submerged vegetation. The landfall locations of two VSCSs are indicated by red dashed arrow with respect to Chilika Lagoon (open circle) (c and d)

connected to the Bay of Bengal (Jayaraman et al. 2005; Panda and Mohanty 2008). The narrowing is mainly resulting from the accumulation of sediment entering through drainage basins surrounding the lagoon (Panigrahi et al. 2009). Approximately 1.5 million tons of sediment per year enters the lagoon from the northern part by the distributaries of the Mahanadi River and 0.3 million tons per year enters the lagoon from the western catchment (Patnaik 1998). Therefore, spatio-temporal monitoring of watershed surface runoff and its associated impact on total suspended sediment (TSS), a proxy of sediment load into the lagoon is of utmost importance for balance and proper management of the lagoon’s ecosystem (Mishra and Gould 2016; Astuti et al. 2018).

Spatio-temporal information on distribution, dynamics, and trend of TSS in a large water body is difficult to obtain from routine *in-situ* monitoring programs because it is a spatially inhomogeneous and highly variable parameter (Dekker et al. 2001). Therefore, remote sensing techniques have been widely used to monitor TSS and other spatially variable optically active constituents (OACs) in the water column such as phytoplankton and cyanobacteria (Mishra et al. 2013, 2014a, b; Wang et al. 2016; Page et al. 2018), and colored dissolved organic matter (CDOM; Chaichitehrani et al. 2013; Ogashawara et al. 2017; Cao et al. 2018). However, the routine use of remote sensing for monitoring sediment dynamics in many environments (e.g., lakes, estuaries, coastal areas) has been limited due to several factors such as characteristics of remote sensing instruments (spatial and spectral resolution), data costs, and the availability of processing software (Miller and McKee 2004). Some studies have demonstrated that data from ocean color satellite sensors, such as National Aeronautics Space Administration (NASA)'s Moderate Resolution Imaging Spectroradiometer (MODIS), represent a cost-effective alternative to the traditional sampling methods (Hu et al. 2004; Miller and McKee 2004; Chen et al. 2007; Doxaran et al. 2009; Mishra and Mishra 2010). Atmospherically corrected MODIS surface reflectance products (e.g., MOD09GQ and MYD09GQ) from both Terra and Aqua satellite are well calibrated with high geolocational accuracy and can be used to monitor water quality parameters both effectively and frequently. For example, Cui et al. (2013) have used these products (MOD09GQ) from Terra and products (MYD09GQ) from Aqua satellite, for long-term monitoring (2001–2010) of suspended sediment concentration in Poyang Lake, China.

There have been few attempts made in the past to use *in-situ* remote sensing data (Rao et al. 1986) and satellite data (Sudhakar and Pal 1993; Pal and Mohanty 2002; Panda and Mohanty 2008) for water quality assessment of Chilika Lagoon. However, TSS concentration was not estimated in those studies. Mohanty and Pal (2001) tried to predict TSS concentration using LISS-I (IRS-IB) data by incorporating soil brightness index (SBI) for mapping TSS concentration but the coefficient used in their algorithm were obtained from other published literature. In addition, IRS data has reduced sensitivity and temporal frequency compared to MODIS data. Gupta (2013) used RESOURCESAT-1 AWiFS data for estimating TSS concentration by implementing chromaticity technique. This algorithm was based on a single date satellite image (26 November, 2003) and it can only predict TSS concentration up to 42 g/m^3 . Further, MODIS data have several advantages over this product including high temporal resolution, high sensitivity (i.e., 12-bit radiometric resolution), cost effectiveness, and most importantly, free from complexities of atmospheric correction which is required for RESOURCESAT-1 AWiFS data.

In this study, both 1-day (MOD09GQ) and 8-days MODIS products (MOD09Q1) from Terra satellite were incorporated for short-term and long-term monitoring of TSS from surface of water column in Chilika Lagoon. The methodology adopted in this study to predict TSS concentration, though empirical in nature, the field data incorporated during TSS model development were from ten different dates, different months, and years. Therefore, the model was not affected by seasonal and temporal bias including changes in solar angles, a major source of uncertainty in remote

sensing data, which makes it applicable in widely varying geographic regions regardless of variation in shape, size, color and type of sediment. To prove that, the TSS model was validated to similar lakes and estuaries in USA, China, and Argentina, by comparing result against published literature. This TSS model can be adopted as a standard procedure to frequently monitor the sediment dynamics in the lagoon because relationship between reflectance and TSS are generally transferable over time for the same geographic location as long as the source of sediment does not vary substantially (Ritchie et al. 2003; Dekker et al. 2002). Miller and McKee (2004) showed that the 645-nm band used in the algorithm provides considerably more detail about the horizontal distribution of suspended sediment than vertical volumetric distribution and that is why the effect of sediment grain size, shape, and texture is minimal at 645 nm band compared to shorter wavelengths. Therefore, the variability in the model performance because of variations in physical properties of the sediment types can be considered negligible.

The overall objective of this chapter is to analyze the trend and spatio-temporal variability of TSS in the lagoon for the last 14 years (2001–2014). The specific objectives are to (1) utilize a relationship established between *in-situ* measurements of TSS and atmospherically corrected reflectance in MODIS band 1 (R_{rs} at 645 nm) for routine application of MODIS 250 m surface reflectance products (MOD09GQ and MOD09Q1) for TSS monitoring, and (2) characterize the seasonal and inter-annual variability of TSS, and the impact of physical and meteorological parameters, and (3) finally a case study showing implication of satellite based TSS and chlorophyll-a (Chl-*a*) models to assess the impacts of natural hazards such as cyclone on water quality of Chilika Lagoon is presented. This case study is based on comparing the impact of two anniversary very severe cyclonic storms (VSCSs): category-5 *Phailin* (12 October, 2013) and category-4 *Hudhud* (12 October, 2014) on the water quality of Chilika Lagoon (Fig. 8.1c–d).

Estuaries, lagoons and surrounding watershed can experience extreme wind velocities, storm surges and rainfall during hurricanes or cyclones, resulting in strong water column mixing, variability in flow regime and modification in local geomorphology (Peierls et al. 2003). These episodic weather events also cause strong sediment re-suspension in the water column (Chen et al. 2009), which may temporarily alter the overall water quality of an aquatic system and associated biological, chemical and geomorphological processes (Miller et al. 2011). In addition, cyclones facilitate substantial nutrient loading from the surrounding areas that can trigger algal blooms, reduce water clarity and increase hypoxic zones in the lakes and estuaries (Peierls et al. 2003; Miller et al. 2006; Paerl et al. 2006). However, the question is “*Do all cyclones produce similar impact on coastal lakes/lagoons? If not, what factors play a role in determining the type of impact? An individual cyclone’s characteristics is obviously one set of factors, what about watershed characteristics and lake optical property? Why some cyclones trigger algal blooms in a lagoon after their passage and some do not?*” These are some of the questions which shaped the framework for this comprehensive case study and we used satellite-based biophysical models and products to answer these questions.

8.2 Materials & Methods

The following workflow diagram summarizes overall process involved in this study to achieve all the objectives mentioned above (Fig. 8.2). The individual components of this workflow are explained in the following subsections.

8.2.1 MODIS Data and Processing

MODIS Terra sensor 250 m spatial resolution data were downloaded from the NASA Goddard Space Flight Centre’s Level 1 and Atmosphere Archive and Distribution System (LAADS) (<http://ladsweb.nascom.nasa.gov/data>) FTP site. Terra satellite passes over Chilika Lagoon typically between 10:00 and 10:30

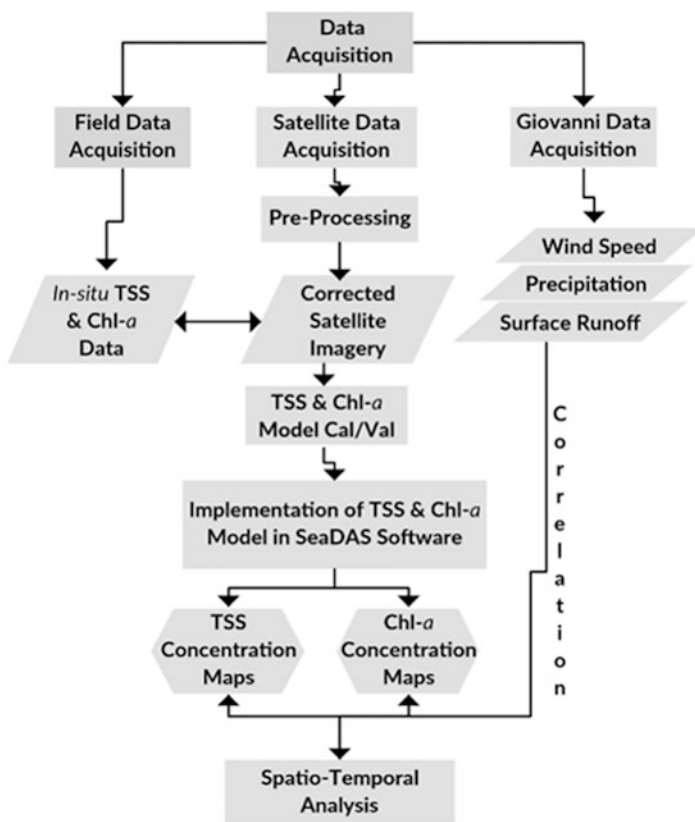


Fig. 8.2 Overall work flow showing individual process involved in this study to produce spatial maps of biophysical products (TSS and Chl-*a*) for spatio-temporal analysis and their variability with physical and meteorological parameters

A.M. local time. For long-term study, MOD09Q1 products covering an entire year were downloaded for 14 years (2001–2014) for weekly and monthly analysis. On the other hand, for assessing differential impacts of two anniversary severe cyclones, MOD09GQ products along with true color images were downloaded corresponding to cyclone months (October 2013 and October 2014). The true colour images were downloaded from NASA's GSFC World view website (<https://earthdata.nasa.gov/labs/worldview/>). High temporal resolution, precise geolocational accuracy and frequent revisit time, make MODIS an ideal satellite sensor to study high-frequency phenomenon such as cyclone impact. The two 250-m bands on MODIS sensor (band 1: 620 nm – 670 nm centered at 645 nm; band 2: 841 nm – 876 nm centered at 859 nm) have sufficient sensitivity to detect a wide range of changes in color of estuarine waters (Hu et al. 2004). Several water quality parameters such as TSS (Miller and McKee 2004; Binding et al. 2005; Chen et al. 2009; Zhang et al. 2010; Zhao et al. 2011; Doxaran et al. 2009; Madrinan et al. 2010; Mishra and Mishra 2010), turbidity (Chen et al. 2007; Petus et al. 2010; Dogliotti et al. 2015), and chlorophyll-a (Mishra and Mishra 2012; Prasad and Singh 2010; Katlane et al. 2012) have been estimated using these two bands. The standard MODIS products (MOD09GQ and MOD09Q1) used in this study contain atmospherically corrected surface reflectance value at bands 1 and 2. MODIS LIB data is used as primary input to obtain MOD09GQ product which is corrected for the effect of gaseous absorption, molecules and aerosol scattering, coupling between atmospheric and surface bi-directional reflectance function, and adjacency effect (Vermote et al. 1997). Doxaran et al. (2009) have described the atmospheric correction process in detail for this product.

To process the MODIS products, Sea viewing Wide Field of view Sensor (SeaWiFS) Data Analysis System (SeaDAS) software available at NASA's ocean colour website (<http://seadas.gsfc.nasa.gov/>) was used. Visual quality check was performed to flag out images with substantive missing data patches and cloud cover. All MODIS images were corrected for spatial distortion by re-projecting them from sinusoidal coordinate system to geographical coordinate system (WGS 84). A geometrical mask was used for extracting the Chilika Lagoon data from all MODIS images. An additional mask, which included a band ratio of remote sensing reflectance (R_{rs}) of band 2 and band 1 ($R_{rs}(859\text{ nm})/R_{rs}(645\text{ nm}) > 1.5$), was used to mask out the islands present inside the lagoon which could not be eliminated using the first geometrical mask.

8.2.2 TSS Model and Long-Term Data Extraction

TSS model (Eq. 8.1) was developed for Chilika Lagoon by Kumar et al. (2016) by re-parameterizing Miller and McKee's linear TSS model (Miller and McKee 2004). The wide range of *in-situ* TSS samples (1.2–161.7 mg/L) from different months and years were used in re-parameterizing the Miller and McKee's TSS model. The calibration result revealed a significant relationship between TSS and the R_{rs}

($R^2 = 0.91$; $n = 54$; $p < 0.001$). In addition to an independent validation (RMSE = 2.64 mg/L; $n = 16$) at Chilika Lagoon, the model was also validated for different geographic locations (Taihu Lake, China; Poyang Lake, China; La-plata River Estuary, Argentina; Mobile Bay Estuary, USA) to test its broad geographic applicability (more details related to TSS model calibration and validation can be found in Kumar et al. 2016).

$$TSS_{Polynomial} = 13181 \times R_{rs}(MODIS B1)^2 - 1408.6 \times R_{rs}(MODIS B1) + 44.15 \quad (8.1)$$

MOD09Q1 data were used for creating TSS concentration maps using above polynomial model (Eq. 8.1) and extracting the weekly mean TSS data to analyze long-term spatio-temporal variability in Chilika Lagoon for 14 years (2001–2014). First, TSS dynamics in the lagoon was visually analyzed for 14 years (2001–2014) at weekly and monthly temporal frequency. MODIS MOD09Q1 product from the first week of months representing different seasons (January, March, May and October) were used to show the TSS spatial distribution patterns in different zones of the lagoon during past 14 years. To demarcate wind induced sediment re-suspension events, wind velocity and direction data were extracted over the Chilika Lagoon from the QuikScat satellite. Further, to quantify more comprehensively seasonal and inter-annual variability in TSS concentration, MODIS data from all months of each year were downloaded for 14 years (2001–2014). For each year, 46 satellite images (MOD09Q1) were downloaded and visualized for quality assessment. TSS model was implemented on cloud free images to derive spatial map products. Some of the images in which the lagoon was partly visible were also used because of a significant lack of cloud free images during monsoon season. Thus, a variation in number of satellite images per year was encountered between years in the long-term spatiotemporal analysis of the TSS. Six sampling points from each sector were used for extracting the TSS concentration from each map product (Fig. 8.1b). Extreme care was taken to avoid interference of emergent and submerged vegetation present in the upper part of northern sector, western part of central sector, and near the boundary of the southern sector. The emergent vegetation in upper part of northern sector were masked completely using a band ratio threshold of 1.5 ($B2/B1 > 1.5$). Similar to Miller and McKee (2004) and Lee et al. (2001), we also assumed that chlorophyll absorption and interference of submerged vegetation has a limited effect on the water leaving radiance at 645 nm (bandwidth: 620–670 nm) because of high attenuation by water itself and contribution from other OACs. In addition, presence of sediment induced turbidity minimizes the bottom reflectance contamination in reflectance data extracted from MODIS pixels and typically carries information from the first few inches of the water surface (Lee et al. 2001; Hu et al. 2004). For each month maximum 4 images were used and the TSS value was averaged to get the mean monthly TSS for each year starting from 2001 to 2014. Seasonal versus inter-annual variability was also compared after analyzing all 14 years TSS data. Finally,

correlation of mean TSS (2001–2014) with different meteorological parameters was carried out for each sector of the lagoon.

8.2.3 *Giovanni Data*

The limited field-based observation of environmental factors invoked the need of satellite sensors and model-derived products. NASA's Giovanni system facilitates access to a range of remote sensing data and other earth science data sets, which helps researchers to implement selected data to a broad area of research field such as terrestrial, atmospheric and marine environment (Acker et al. 2014). It includes data from various NASA missions and projects. To analyze the effect of physical and meteorological forcing on the TSS variability in the lagoon, total surface precipitation and surface runoff data were downloaded from NASA's Giovanni database (<http://giovanni.gsfc.nasa.gov/giovanni/>). MATMNXLND 5.2.0 products from MERRA monthly history data collection were used for the specified catchment area of Chilika Lagoon. Result for each month was visualized from 2001 to 2014 and corresponding NetCDF file of each transect was downloaded for further analysis. The units of the variables were converted from $\text{kg/m}^2/\text{s}$ to $\text{g/m}^2/\text{day}$ using a multiplication factor of 86,400,000 to incorporate in the SeaDAS statistical tool. Further, three geometrical masks were used for analyzing the catchment area separately, northern (N) catchment ($20^\circ \text{N} - 20^\circ 48' \text{N}$, $85^\circ \text{E} - 86^\circ 24' \text{E}$), western (W) catchment ($19^\circ 24' \text{N} - 20^\circ \text{N}$, $84^\circ \text{E} - 85^\circ \text{E}$), and overall catchment. Monthly average value was estimated for different catchment areas using corresponding geometrical masks. In addition, monthly wind stress magnitude data were also downloaded directly using Giovanni-4 seasonal time series plot for catchment area to complement precipitation and runoff data in the long-term analysis of TSS variability in the lagoon.

Further, to assess cyclone impact, high temporal frequency data was required. Therefore, 3-h Tropical rainfall measuring mission (TRMM) precipitation products (TRMM_3B42RT.007) were downloaded to capture the highest rainfall event around the lagoon catchment on the landfall day of the two VSCSs (*Phailin* and *Hudhud*). TRMM data from Giovanni was also used by Acker and Leptoukh (2007) to show the rainfall accumulation during Hurricane *Ivan* (16 September, 2004) around Gulf of Mexico, Florida and Alabama. In addition, Global Land Data Analysis System (GLDAS) was also used for visualising the GLDAS-derived rainfall rate, surface runoff and near-surface wind speed products to capture the surface level alteration, especially for analysing the variability in the catchment of the lagoon, caused by the anniversary cyclones. GLDAS is an interactive programme which incorporates both satellite and ground based observations at a spatial resolution of $0.25 \times 0.25^\circ$ (Fox and Rowntree 2013). Rodell and Houser (2004) and Fang et al. (2008) have described about GLDAS products in detail in their studies. In this study, the 3-hourly product (GLDAS_NOAH025SUBP_3H.001) was used for analysing the short-term variations in physical (surface runoff) and meteorological (rainfall rate and wind speed)

parameters. Further, data were time averaged to generate 1-day averaged data for all the physical and meteorological parameters. These products are based on NOAA model (http://disc.sci.gsfc.nasa.gov/datacollection/GLDAS_NOAH025_3H_V020.shtml). NOAA model incorporate near surface atmospheric forcing data as input such as soil moisture, soil temperature, canopy water content, energy flux and water flux terms of surface energy balance and water energy balance for simulation.

8.2.4 Differential Impact Analysis of Anniversary Cyclones: A Case Study

8.2.4.1 VSCSs Characteristics

Figure 8.3a shows the trajectories of VSCSs *Phailin* and *Hudhud*. *Phailin* struck the Odisha coast on October 12, 2013 around 22:30 h Indian Standard Time (IST) (17:00 h UTC) with the maximum wind velocity reaching up to 220 km/h (IMD 2013). This VSCS was classified as category 5 on the Saffir-Simpson scale as per the norms of National Oceanic and Atmospheric Administration (NOAA). It was the second strongest tropical cyclone in the recorded history to make landfall in India only after the super cyclone of Odisha which struck the same area in 1999 with wind speed up to 260 km/h (IFRC 1999). Initially, a low pressure was formed in South China Sea on October 06, 2013 which further intensified into cyclonic storm on October 09, 2013 moving west-northwestwardly. It further intensified into a VSCS by moving northwestwardly on October 10 and finally made landfall on October

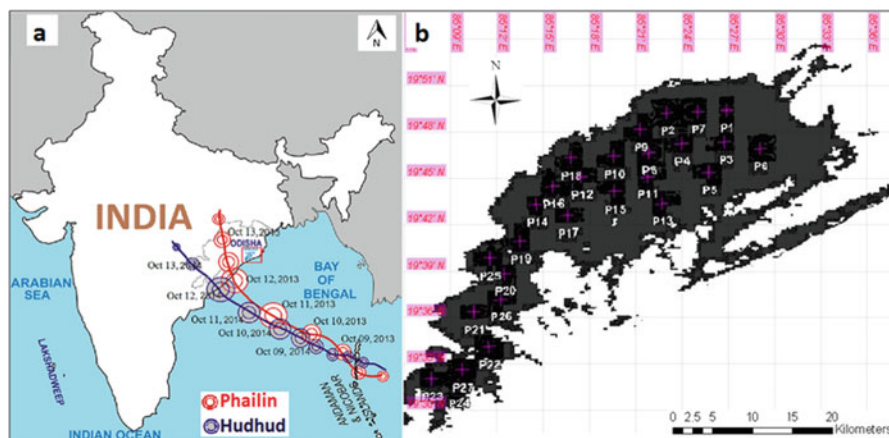


Fig. 8.3 Track of the two VSCSs (*Phailin*: red line and *Hudhud*: blue line) with respect to Chilika Lagoon (a). MODIS image (MOD09GQ) with random sampling locations (Total 27 random pixel locations ($n = 27$): 9 from each sector (NS, CS, and SS)) were used for quantitative analysis of TSS and Chl-*a* in different sectors of the lagoon for differential impact assessment of anniversary cyclones on the water quality of Chilika Lagoon (b)

Table 8.1 Comparative description of anniversary VSCSs (*Phailin* and *Hudhud*)

Parameters	<i>Phailin</i>	<i>Hudhud</i>
Origin location with date	Gulf of Thailand and adjoining North Andaman Sea (October 6, 2013) (9.5° N, 102.00° E)	Tenasserim coast and adjoining North Andaman Sea (October 6, 2014) (10° N, 96° E)
Landfall location	Gopalpur, Odisha (19.27° N, 84.92° E)	Visakhapatnam, Andhra Pradesh (17.69° N, 83.22° E)
Distance (direction) from Chilika	45 km (southwest of Chilika)	338 km (southwest of Chilika)
Duration (stay over land)	~5 days	~3 days
Landfall date with time	October 12, 2013 (22:30 IST)	October 12, 2014 (between 12:00 and 13:00 IST)
Category	Category-5	Category-4
Wind speed (maximum)	215 km/h (115 Knots)	185 km/h (100 Knots)
Rainfall near lagoon (landfall day)	160 mm	80 mm
Central pressure (minimum)	940 hPa	950 hPa
Pressure drop (maximum)	66 hPa	54 hPa
Storm surge (maximum)	2–2.5 m above astronomical tides	1.4 m above astronomical tides
Economic impact	USD \$696 million	USD \$3.4 billion
Total number of fatalities	45	124

The data were collected from reports of central and state government organisation (IMD 2013, 2014; GoO 2013)

12 near Gopalpur district in Odisha (IMD 2013). The landfall location of VSCS *Phailin* was only 45 km southwest from Chilika Lagoon. The landfall of *Phailin* brought torrential rain and storm surges up to 3.5 m to the eastern Indian states of Odisha and Andhra Pradesh (UNEP 2013). Important characteristics of both VSCS are presented in Table 8.1.

The second VSCS *Hudhud*, made landfall on October 12, 2014 near Visakhapatnam, Andhra Pradesh, exactly 1 year after VSCS *Phailin*. The landfall location was at a distance of 338 km southwest from Chilika Lagoon. This tropical cyclone was categorized as category 4 cyclone on the Saffir-Simpson scale. The maximum sustained wind speed during its landfall was about 185 km/h (IMD 2014). These VSCSs, *Phailin* and *Hudhud*, were very similar in their characteristics as both originated in the North Andaman Sea and moved almost in parallel path but there was a relatively small difference in strength, wind speed, landfall location, and passage

within the catchment after the landfall (Table 8.1; Mishra and Panigrahi 2014). Both VSCSs produced high negative economic impact, and a large number of fatalities reported only during VSCS Hudhud compared to VSCS Phailin as it struck the areas with high population densities and larger cities (Table 8.1) (IMD 2013, 2014).

8.2.4.2 Differential Impact on TSS and Chl-*a*

MODIS true colour images corresponding to pre-VSCSs (7 October, 2013 and 2014: the nearest cloud-free image before the landfall of cyclones), landfall day (12 October, 2013 and 2014) and post-VSCSs (14 October, 2013 and 2014) were incorporated to show the differential change in water colour of the Chilika Lagoon and its surrounding region. However, MODIS 1-day revisit period limited its applicability for tracking the duration and path of cyclone on an hourly basis. Thus, we incorporated Giovanni-derived three-hourly rainfall and surface runoff transects on landfall day to show the track, duration and the maximum area of impact caused by both VSCSs. Data extracted from Giovanni transects corresponding to surface wind speed, rainfall rate and surface runoff for the catchment area of the lagoon was compared daily for the month of October, 2013 and 2014. Each of the 3-h products were time averaged for 24 h using Giovanni's time averaged map tool (<http://giovanni.sci.gsfc.nasa.gov/giovanni/>) and the averaged transect files were downloaded in NetCDF format. Further, a geometrical mask was used to extract the time averaged data corresponding to the catchment area of the lagoon.

The ultimate objective of this case study was to evaluate the differential impacts of VSCSs on the biophysical parameters that govern the water quality of the lagoon. To accomplish the objective, TSS and Chl-*a* concentration were extracted from 27 locations (P1-P27) marked in Fig. 8.3b using MOD09GQ data. Nine locations from each sector; NS (P1-P9), CS (P10-P18), and SS (P19-P27) were randomly selected to extract the TSS and Chl-*a* concentration in the lagoon pre- and post VSCSs. TSS and Chl-*a* spatial maps were created using MODIS based TSS model (Kumar et al. 2016) and Chl-*a* slope model respectively (Srichandan et al. 2015) (Eq. 8.2), both developed recently for Chilika Lagoon. The slope model was developed with the *in-situ* Chl-*a* samples corresponding to the cyclone month (October 2013). A significant relationship ($R^2 = 0.59$; $n = 29$; $p < 0.001$; $RMSE = 20.7\%$; $bias = 8.4\%$) was established between *in-situ* Chl-*a* concentration and slope of MODIS band 3 and band 4 as follows:

$$\text{Chl } a = 211.98 * \exp (6320.3 * \text{Slope Reflectance}) \quad (8.2)$$

where,

$$\text{Slope Reflectance} = \frac{R_{rs} (B3) - R_{rs} (B4)}{|\text{Band Center}(B3) - \text{Band Center} (B4)|} \quad (8.3)$$

$$\text{Reflectance(Band 3)} = 0.4796 * \text{Reflectance (Band 1)} + 0.0189 \quad (8.4)$$

$$\text{Reflectance (Band 4)} = 0.7186 * \text{Reflectance (Band 1)} + 0.0407 \quad (8.5)$$

A similar slope model was used to derive Chl-*a* concentration from MODIS data from Lake Pontchartrain, Louisiana, USA (Mishra and Mishra 2010). Accuracy was a major factor for selecting these published TSS and Chl-*a* models because both were calibrated and validated with *in-situ* samples from Chilika Lagoon itself. The accuracy of Chl-*a* model implemented in this study was compared with four other published models (Gitelson et al. 2003; Kahru et al. 2004; Zhang et al. 2011; El-Alem et al. 2012), and it was found to perform better compared with others (more details can be found in Srichandan et al. 2015). Finally, TSS and Chl-*a* maps were created and placed side by side to demarcate the spatio-temporal variation in these parameters pre- during post- VSCS periods.

8.3 Results and Discussion

8.3.1 Long-Term Trend of TSS- Visual Analysis

TSS composite from first week of different months representing different season (January, March, May, and October) were used to analyse the trend in inter-annual and seasonal variability (Fig. 8.4). From the qualitative analysis of these time-series TSS products, it was observed that the TSS concentration in northern sector have been consistently higher than that of the other two sectors except in summer (May) (Fig. 8.4). As the river discharge during this period remains low, high TSS throughout the lagoon in May could be due to the wind-induced sediment re-suspension events since wind speed was observed to be the highest during summer months (Bramha et al. 2008).

October is the month following the south-west monsoon (June-Sept) and April is the pre-monsoon period. Therefore, the influx of fresh water through the riverine system and land drainage to the lagoon is maximum during October and minimum during April (Pal and Mohanty 2002). This is the main reason for relatively low concentration of TSS observed in northern sector of the lagoon during pre-monsoon period (i.e., in March) (Fig. 8.4b). The central sector has shown intermediate variations in TSS concentration for different seasons as compared to other two sectors. This could be mainly due to less number of rivers connecting to this sector as compared to northern sector and comparatively more number of rivers than southern sector.

TSS concentration in the southern sector of the lagoon was generally lower as compared to other two sectors, except in the month of May (Fig. 8.4). Low depth and churning action of water by southerly wind is the primary cause of re-suspension of fine sediments from bottom during the month of May and increasing turbidity in the southern sector (Bramha et al. 2008). Chen et al. (2007) found that wind velocity and

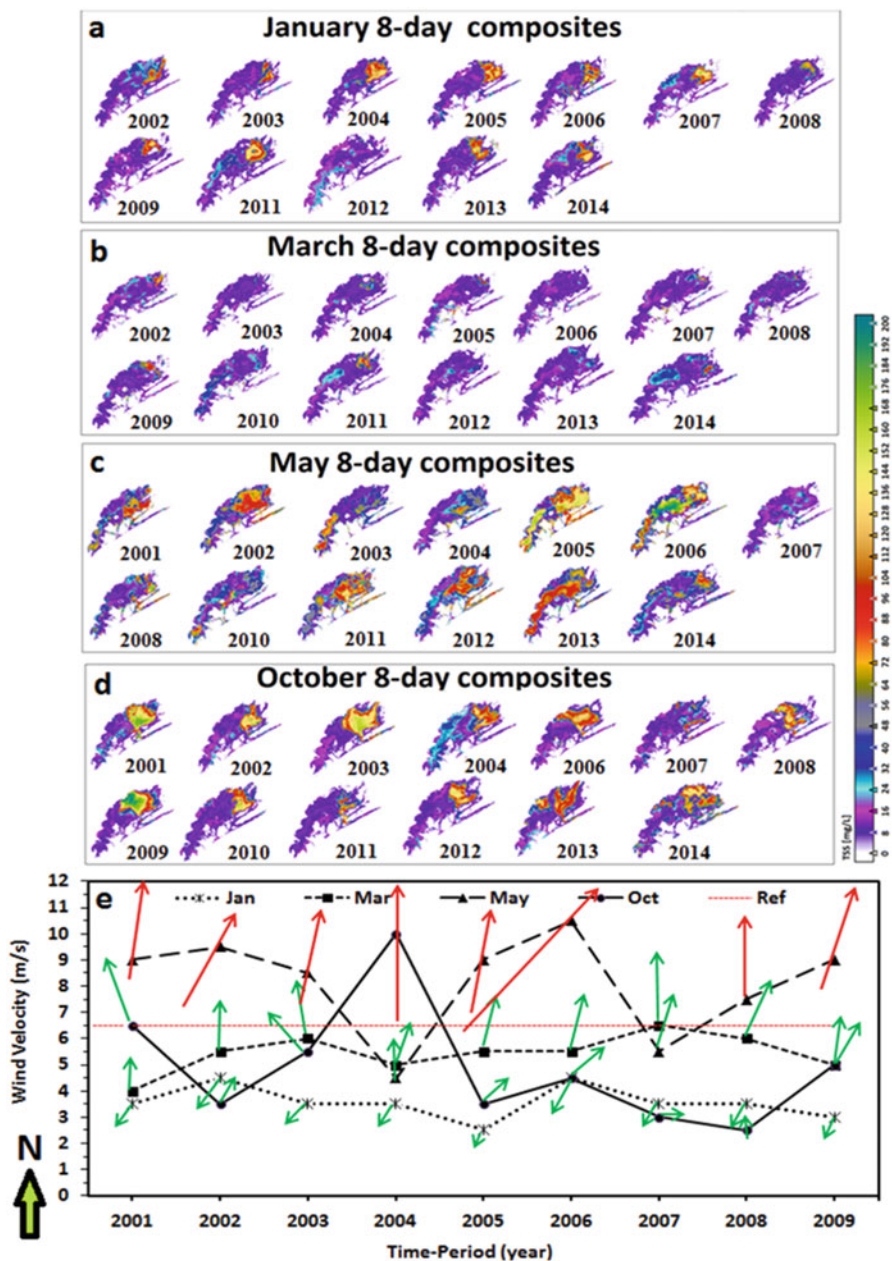


Fig. 8.4 Spatio-temporal distribution of TSS over Chilika Lagoon with MODIS 8-day composite images in different seasons across the years (**a**, **b**, **c**, and **d**). First week images were used for comparison as most of the images were found to be cloud free during this period. The gap in years among images indicates the lack of cloud free images for those years (**a**, **b**, **c**, and **d**). In addition, first week averaged wind velocity with direction derived from QuikScat for Chilika Lagoon

direction can play a major role in increasing the overall turbidity in water bodies particularly in the shallow areas through the re-suspension of bottom sediments. Zhao et al. (2011) described the event of re-suspension in shallow Mobile Bay estuary, Alabama using two MODIS images captured within the time gap of 2-days. To delineate the re-suspension event in this study, wind speed data from the QuikScat satellite were analyzed over the Lagoon for the first week of each month as shown in Fig. 8.4e.

It was observed that during summer (May), wind direction remains predominantly southerly and southwesterly over the lagoon, however, during winter (January), wind direction is either northerly or north-easterly (Fig. 8.4e). The wind direction results were found to be consistent with previous studies (Bramha et al. 2008; Mohanty and Panda 2009). It was observed that typically wind velocity during the month of May was high ($8\text{--}10\text{ ms}^{-1}$) as compared to other months and direction of wind was from south-west to north-east. In May 2004 and 2007, when average wind speed was below 6.5 ms^{-1} , inter-annual turbidity levels in the lagoon were the lowest because of the lack of sediment re-suspension events (Fig. 8.4c, e). However, when the average wind speed was more than 6.5 ms^{-1} in May during other years, re-suspension of sediment particularly in shallow areas increased the overall turbidity level. This threshold value (6.5 ms^{-1}) was chosen by observing TSS variability during October 2001 when slight resuspension was observed in southern sector at 6.5 ms^{-1} . Zhang et al. (2010) have also suggested that wind speed in the range of $5\text{--}6\text{ ms}^{-1}$ is always critical for resuspension events and they used $>6\text{ ms}^{-1}$ as reference for Lake Taihu, China. The effect of re-suspension of bottom sediments in southern sector of the lagoon is clearly visible (Fig. 8.4a–d). Interestingly, during October (post-monsoon) 2004, the only October between 2001 and 2009, the wind exceeded the 6.5 ms^{-1} threshold reaching up to 10 ms^{-1} , sediment re-suspension event was observed throughout the lagoon in addition to the normal post-monsoonal river discharge induced high turbidity in the northern sector (Fig. 8.4e, d).

8.3.2 Long-Term Trend of TSS- Quantitative Analysis

To analyze the influence of precipitation and surface runoff on TSS in the lagoon, a comparative analysis was performed between the two major catchments, the northern (N) and the western (W) catchment (Fig. 8.5). Results for overall catchment area were also analyzed. It was observed that although the magnitude of precipitation in both catchment areas (N and W) was very similar, runoff from N catchment was



Fig. 8.4 (continued) corresponding to the months incorporated in long-term trend of TSS-visual analysis (e). The 6.5 ms^{-1} (dashed red line) indicates threshold limit for re-suspension induced turbidity and red arrow indicates wind speed above threshold limit while green arrows are below threshold limit (e)

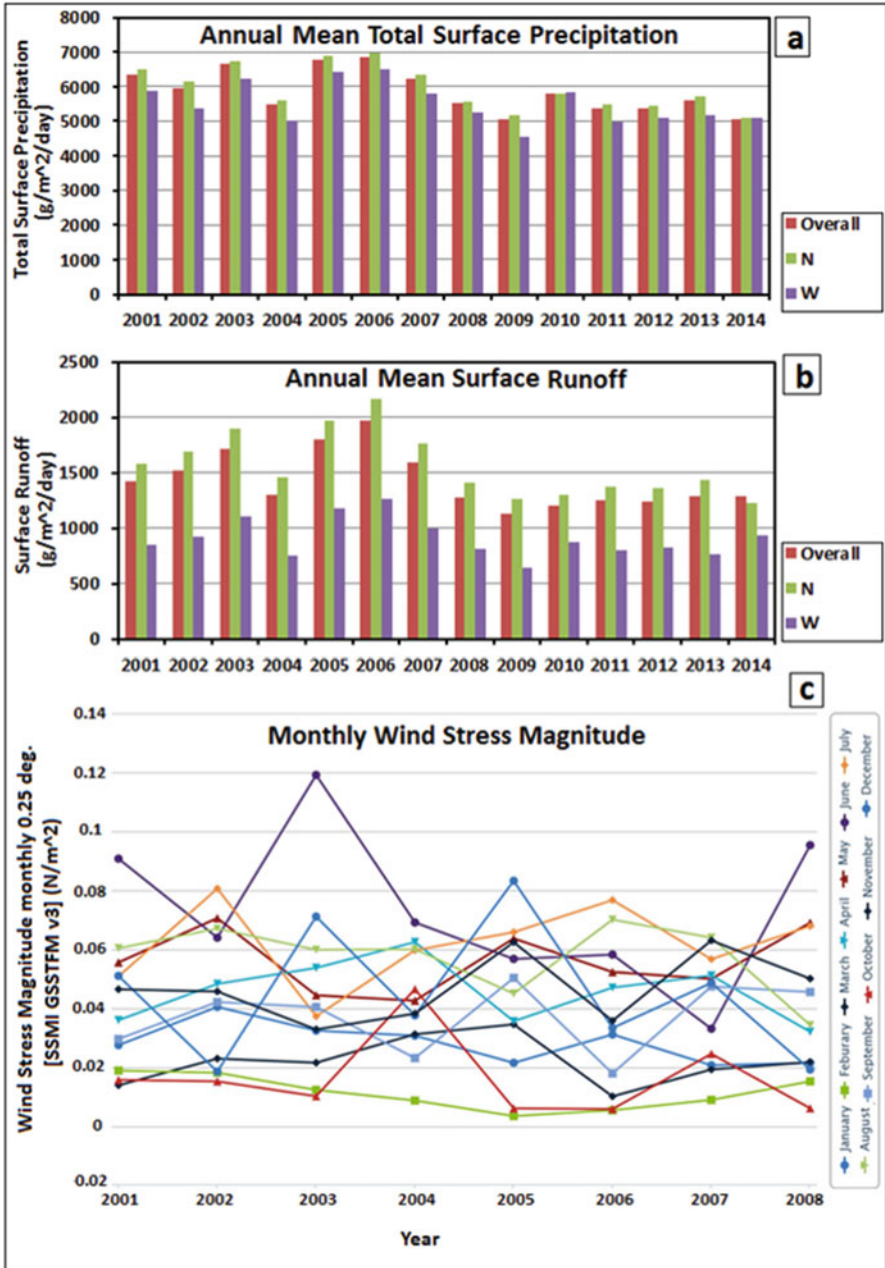


Fig. 8.5 Temporally and spatially averaged magnitude of meteorological and physical parameters: total surface precipitation (a); surface runoff (b) and wind stress magnitude (c) over the catchment area of Chilika Lagoon. N & W represents northern (20° N – 20°48' N, 85° E – 86°24' E) and western (19°24' N – 20° N, 84° E – 85° E) catchment area. Overall catchment used for analysis covered area between 19°24' N – 20°48' N, 84° E – 86°24' E

observed to be 24.69–49.59% (2014 and 2009 respectively) more than from the W catchment area (Fig. 8.5a, b).

The significant difference in runoff is mainly due to the large number of rivers and rivulets flowing into the lagoon from the north (Fig. 8.1a). Further, heavy forest cover in the western catchment may be playing a role in reducing the surface runoff. The above finding further justified the reason behind consistently higher TSS concentration in northern sector of the lagoon compared to central and southern sector. In addition to precipitation and runoff, monthly wind stress magnitude from Giovanni is shown in Fig. 8.5c. The monthly wind stress generated from Giovanni-4 seasonal time series plot (<http://giovanni.gsfc.nasa.gov/>) specified that during pre-monsoon (April, May) and monsoon (June, July and August) wind magnitude remain high (Fig. 8.5c) which plays major role in re-suspension of sediment mostly during pre-monsoon period as discussed in earlier section (visual analysis).

The mean TSS concentration data was obtained for each month and each sector. TSS data were extracted and averaged from pixel locations shown in Fig. 8.1b which covered the entire lagoon. Table 8.2 shows the complete statistics of the long-term analysis result on a monthly basis in different sectors of the lagoon from 2001 to 2014. There are variations in the number of satellite images used for different months mainly due to factors such as image quality and cloud cover. Maximum cloud cover was encountered during the monsoon (June, July, and August) which were also the months when precipitation and surface runoff were maximum. During the 14 years (7975 pixels), the minimum predicted TSS concentration was 6.54 mg/L which is the lower limit for the prediction model (Table 8.2). The highest TSS concentration was recorded during July 2006 (NS: 860.22 mg/L; CS: 435.94 mg/L; SS: 371.91 mg/L) due to the combination of maximum precipitation (17341.03 g/m²/day), runoff (8019.735 g/m²/day), and wind speed during monsoon of 2006, mainly in July. It clearly indicates the influence of these three factors in controlling the TSS dynamics in the lagoon. Overall concentration of TSS remained high during June, July, and August each year in all the sectors of the lagoon mainly due to heavy rainfall and high surface runoff during those months.

The monthly average of each parameter for 14 years, except wind stress (8 years), showed the dominance of monsoon induced precipitation, runoff, and wind stress and associated high TSS (Fig. 8.6a). The effect of precipitation and associated runoff on TSS was much more pronounced in NS followed by CS and SS (Fig. 8.6b). In addition, central and southern parts of the lagoon consistently experience the settling of sediment at a faster rate during post-monsoon period compared to the NS. This could be due to a combination of generally higher runoff and post-monsoon wind direction from north-east to south-west supporting the re-suspension event in NS of the lagoon.

Correlation analysis between monthly average TSS and precipitation and surface runoff for different sectors is shown in Fig. 8.6c–h. As observed in Fig. 8.6b, the TSS in the NS and CS of the lagoon is highly correlated with total precipitation (R^2 : 0.852 and 0.927 for NS and CS respectively) and surface runoff (R^2 : 0.910 and 0.772 for NS and CS respectively). However, TSS in the SS of the lagoon is weakly correlated with precipitation (R^2 : 0.4295) and surface runoff (R^2 : 0.1876) (Figs. 8.6c, d, e).

Table 8.2 Descriptive statistics showing the long-term (2001–2014) variability of TSS (mg/L) in different sectors of the lagoon

Sector	Statistics	Jan	Feb	Mar	Apr	May	Jun	Jul	Aug	Sep	Oct	Nov	Dec
NS	Min	6.55	6.54	6.55	6.55	6.63	7.61	15.87	13.39	6.55	6.55	6.54	6.55
	Max	172.16	113.05	230.64	217.77	270.79	226.54	860.22	530.05	431.67	276.81	200.77	185.72
	Mean	50.51	24.89	26.38	44.55	68.81	89.66	182.51	206.86	138.15	89.87	75.49	70.61
	Std. dev.	41.44	23.16	31.71	37.89	48.39	64.12	171.85	105.73	79.13	48.68	43.39	46.25
	Std. error	2.49	1.31	1.84	2.38	3.31	7.61	21.15	7.69	5.19	3.03	2.48	2.78
	N	276	312	298	253	213	71	66	189	232	257	306	276
CS	Min	6.55	6.55	6.54	6.55	6.55	6.58	6.56	6.55	6.54	6.55	6.54	6.55
	Max	52.26	64.99	251.38	149.63	355.42	220.79	435.94	464.47	462.99	206.9	122.49	104.24
	Mean	12.48	13.05	17.79	32.11	50.64	67.06	112.99	105.77	63.47	30.57	15.51	14.01
	Std. dev.	7.23	8.13	27.44	33.64	51.83	56.67	109.61	105.98	76.82	38.82	15.43	12.03
	Std. error	0.43	0.46	1.59	2.15	3.64	6.77	13.92	8.45	5.06	2.52	0.88	0.72
	N	272	312	295	243	202	70	62	157	230	237	304	273
SS	Min	6.54	6.55	6.55	6.55	6.55	6.56	7.49	6.59	6.55	6.55	6.54	6.54
	Max	34.91	41.77	204.96	185.72	167.46	236.18	371.91	186.64	211.48	52.57	30.37	44.15
	Mean	10.01	10.26	20.09	42.87	50.62	56.42	90.56	37.62	18.34	15.56	10.27	10.33
	Std. dev.	4.99	5.13	26.01	34.77	36.55	58.71	91.47	44.69	17.03	9.34	4.73	5.26
	Std. error	0.31	0.29	1.53	2.21	2.51	7.28	12.01	4.09	1.18	0.62	0.27	0.31
	N	270	303	286	248	212	65	58	119	206	223	305	274
Total no. of images used		47	52	50	43	37	12	11	33	41	43	51	46

Out of 46 MODIS 8-day composites (MOD09Q1) each year i.e. 644 images, total number of satellite images used for analysis was 466 and rest were discarded due to poor quality and cloud cover. The total number of MODIS pixels (N) used for TSS data extraction is 7975

This variation in the magnitude of correlation is mainly due to the variation in number of tributaries connecting to the different sectors of the lagoon as they act as the primary transporting medium controlling runoff into the lagoon. Wind stress magnitude on the other hand showed high correlation (R^2 : 0.54) with mean TSS in SS compared to CS (R^2 : 0.18) and NS (R^2 : 0.42). The predominant direction of wind is from south and south-west to north and north-east during summer and that along with shallow depth in the SS could be the main reasons why that sector experiences more intense re-suspension events compared to other sectors.

Temporal variation of R^2 between TSS and above factors for different sectors was also assessed to cross validate the correlation analysis (Fig. 8.6f, g, h). The results indicated that NS of the lagoon was steadily well correlated with precipitation and runoff for all years (Fig. 8.6f). Also, CS was strongly correlated with runoff and precipitation though there was drastic drop in R^2 value for the year 2002 and 2010 (Fig. 8.6g). That was possibly caused due to the anomalously high wind speed (Figs. 8.3c and 8.4e) observed during May, 2002 which triggered a re-suspension event. A similar phenomenon was also observed in 2010. In the SS region, the TSS showed better correlation with wind speed compared to other two factors (runoff and precipitation) during the period (2001–2008), except for some years (2007 and 2008) (Fig. 8.6h). In general, it can be concluded that the spatio-temporal variability of TSS in different sectors of the lagoon is controlled by different environmental forcings and the pattern of variability in different sectors was observed to be similar (i.e. high in NS, moderate in CS, and low in SS) over the 14 years. However, the seasonal (monthly) variability is stronger compared to inter-annual variability for all parameters (TSS, precipitation, runoff, wind stress). Descriptive statistics of monthly and inter-annual variability in mean TSS concentration is provided in Table 8.3. It is apparent from the Table 8.3 that monthly (seasonal) variation in mean TSS for different sectors of the lagoon (Standard deviation: NS-58.36 mg/L, CS-35.92 mg/L, SS-25.24 mg/L) are very high compared to inter-annual variation (Standard deviation: NS-12.27 mg/L, CS-9.49 mg/L, SS-6.81 mg/L). Annual variability plot also highlighted the fact that TSS concentration is significantly more in NS compared to CS and SS (Fig. 8.6b).

8.3.3 Differential Impact Analysis of Anniversary Cyclones

MODIS true color images prior to both VSCSs indicated the usual turbidity regime of the lagoon as discussed earlier i.e., high turbidity in NS due to heavy freshwater influx and comparatively low turbidity in CS and SS (Fig. 8.7a–b). One important difference observed in true color images was that prior to *Phailin*, land pixels of the MODIS image appeared darker compared to pre-*Hudhud* (Fig. 8.7a–b). Also, the BOB appeared more turbid (light blue) in pre-*Phailin* MODIS image (Fig. 8.7a) compared to the pre-*Hudhud* image (dark blue) (Fig. 8.7b). The reason behind this difference is most likely the ~threefold high rainfall during the beginning of October 2013 (1st week total precipitation: 1.46 kg/m² for overall catchment 19.4° N – 20.4° N and 84.6° E – 85.8° E) compared to initial period of October 2014 (1st week total

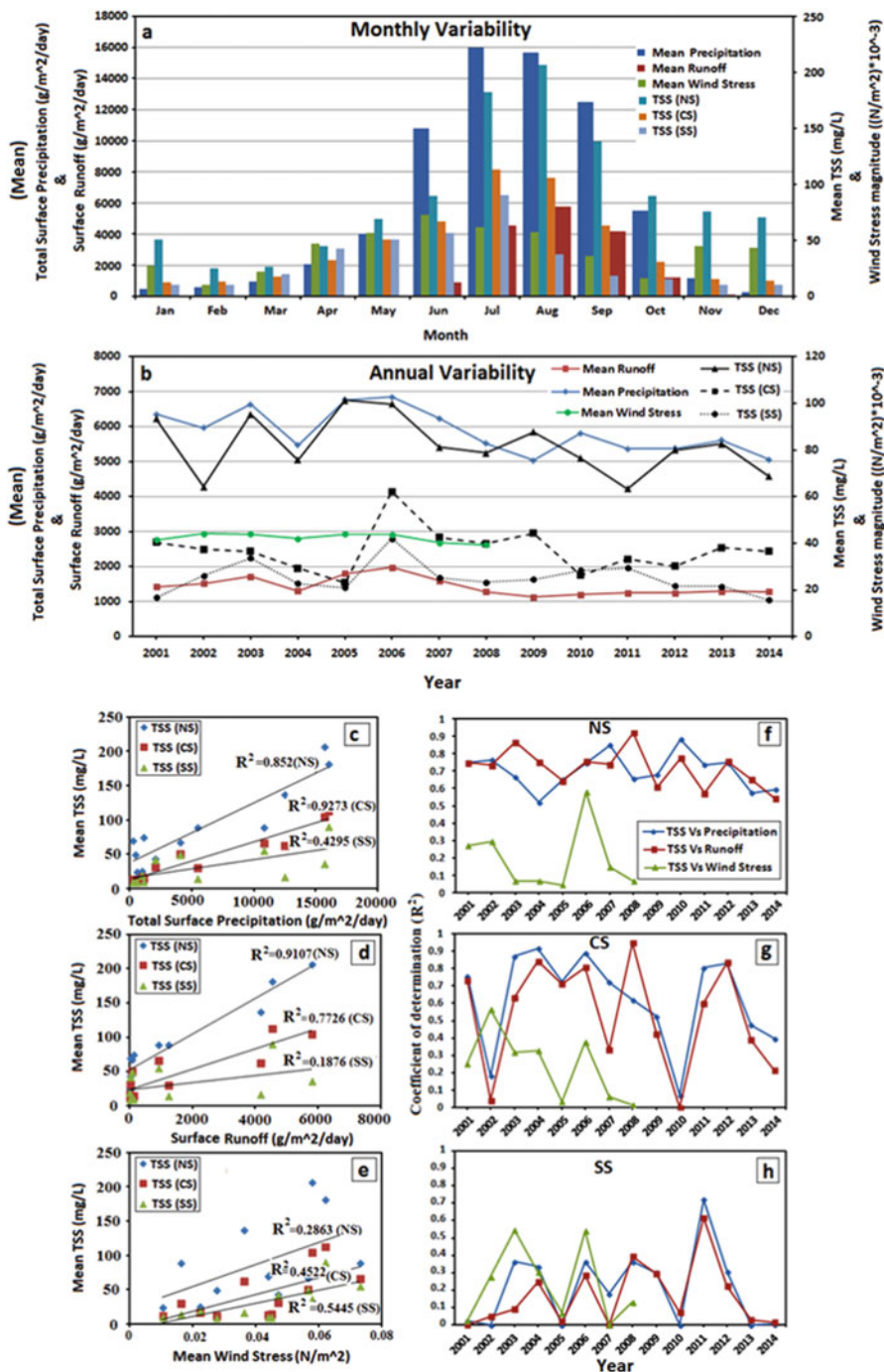


Fig. 8.6 Monthly (January–December) (a) and annual (2001–2014) (b) variability of various parameters (precipitation, runoff, wind Stress, and TSS) for Chilika Lagoon. Temporal variability

Table 8.3 Statistical comparison between seasonal and inter-annual variability in mean TSS concentration for different sectors of Chilika Lagoon from 2001 to 2014

Statistics mean TSS (mg/L)	NS		CS		SS	
	Monthly	Annual	Monthly	Annual	Monthly	Annual
Minimum	24.89	63.28	12.48	23.07	10.01	15.69
Maximum	206.86	101.29	112.99	62.21	90.56	42.03
Range	181.97	38.01	100.51	39.14	80.55	26.34
Std. deviation	58.36	12.27	35.92	9.49	25.24	6.81

precipitation: 0.55 kg/m^2 for the same catchment) that made the land surface saturated and appeared darker and also increased runoff to BOB making it more turbid. Angles et al. (2015) suggested that the environmental condition pre-and post-cyclone will primarily determine its impact on estuaries and lagoons. The landfall day image of VSCS *Phailin* revealed that its swath covered the entire Chilika Lagoon and its eye was clearly demarcated close to the lagoon (Fig. 8.7c). On the other hand, the outer band of VSCS *Hudhud* covered the Chilika Lagoon and its eye was comparatively at a larger distance from the lagoon (Fig. 8.7d). Chilika Lagoon appeared completely turbid (brown color) in post-*Phailin* MODIS image and a large sediment plume is also apparent that extended towards the BOB due to flooded river extracts (Fig. 8.7e). The flood intensity in Rushikuliya River below the Chilika Lagoon can be observed easily in MODIS images post-*Phailin* (Fig. 8.7e). In contrast, the post-*Hudhud* MODIS images revealed lesser impact on Chilika Lagoon in terms of turbidity levels, particularly in CS and SS, based on the visual analysis of the water color in MODIS true color data. Also, the spatial extent of the sediment plumes in BOB appeared a little thinner most likely due to comparatively lesser river discharge (Fig. 8.7f).

The path of both VSCSs and how long their impact lasted around the Chilika Lagoon can be observed in the 3-hourly Giovanni derived TRMM transects (Fig. 8.8). Previous studies discussed that characteristics of a cyclone such as landfall location, intensity, trajectory, speed of passage, are some of the important factors which can produce significantly different impact (Mallin et al. 2002; Mallin and Corbrett 2006; Srichandan et al. 2015). There was continuous rainfall observed over or near Chilika Lagoon (indicated by open circles in Figs. 8.8a–h) for 24 h on the landfall day of *Phailin*. In contrast, transects corresponding to landfall day of *Hudhud* revealed that the precipitation over or near the lagoon lasted only for 9–12 h (Fig. 8.8i–p). Swath of both the VSCSs and their progress can be observed in these transects. The landfall points of *Phailin* (Gopalpur) and *Hudhud* (Visakhapatnam)



Fig. 8.6 (continued) in mean TSS is shown by different symbols and color bar for different sectors (NS, CS and SS). Correlation between average TSS concentration for different sectors (NS, CS and SS) and meteorological and physical parameters (precipitation, surface runoff and wind stress) (c, d, and e). The mean value of each parameter for each month was averaged for 14 years (2001–2014) and correlated with mean TSS value for different sectors. Temporal variation is also shown in the form of R^2 for different sectors (f, g, and h)

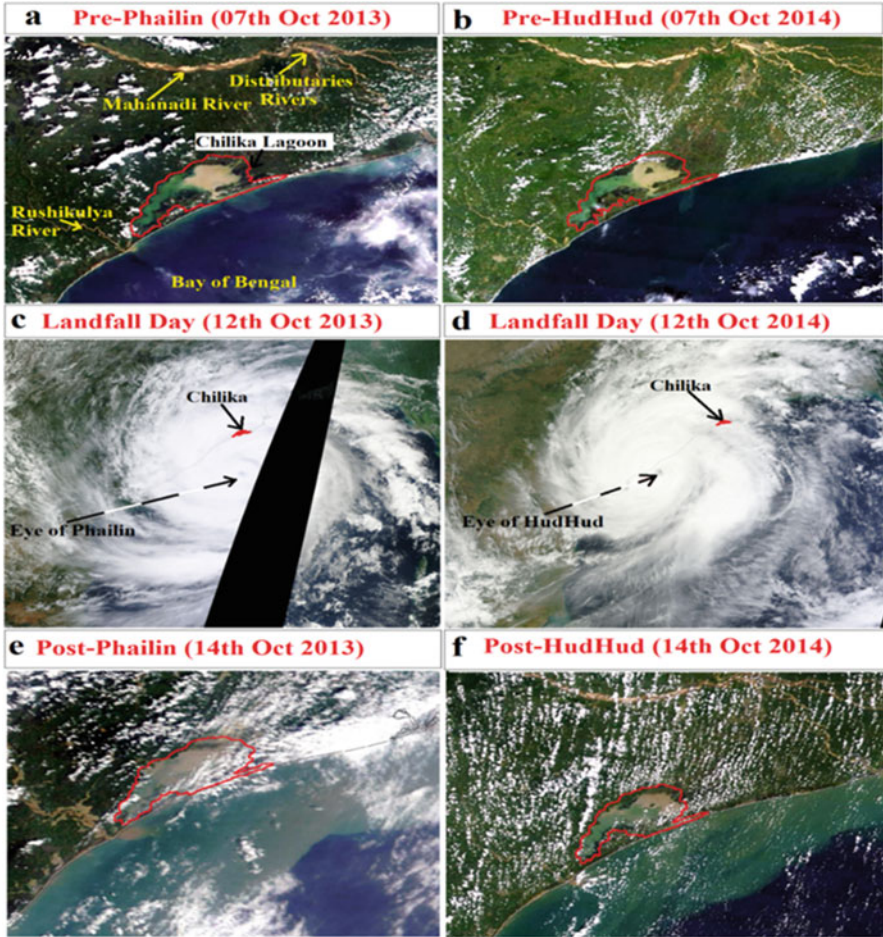


Fig. 8.7 Visual analysis of the impacts of VSCSs *Phailin* and *Hudhud* on Chilika Lagoon and surrounding region using MODIS true color images: pre-*Phailin* (a), pre-*Hudhud* (b), landfall day of *Phailin* (c), landfall day of *Hudhud* (d), post-*Phailin* (e), post-*Hudhud* (f). Chilika Lagoon is demarcated by the red polygon and the distributaries of Mahanadi River (major source of freshwater for the lagoon) connecting the lagoon are marked by solid arrow (a). The eyes of both cyclones are indicated by dashed arrow (c–d)

are shown by dashed arrows with respect to Chilika Lagoon (solid arrow) (Fig. 8.8g, l). The 24-h analysis revealed very high average rainfall (~100–110 mm) near the lagoon during *Phailin* compared to *Hudhud* (~55–60 mm).

The precise effect of heavy rainfall around Chilika Lagoon is further revealed by the 3-hourly surface precipitation and surface runoff transects (Fig. 8.9). 3-hourly surface runoff transects showed a close temporal matching with high rainfall locations (Fig. 8.9a–p, a’–p’). As suspected, the 24 h comparative result shown in Fig. 8.9q–r indicated high surface runoff during *Phailin* (NC: highest up to

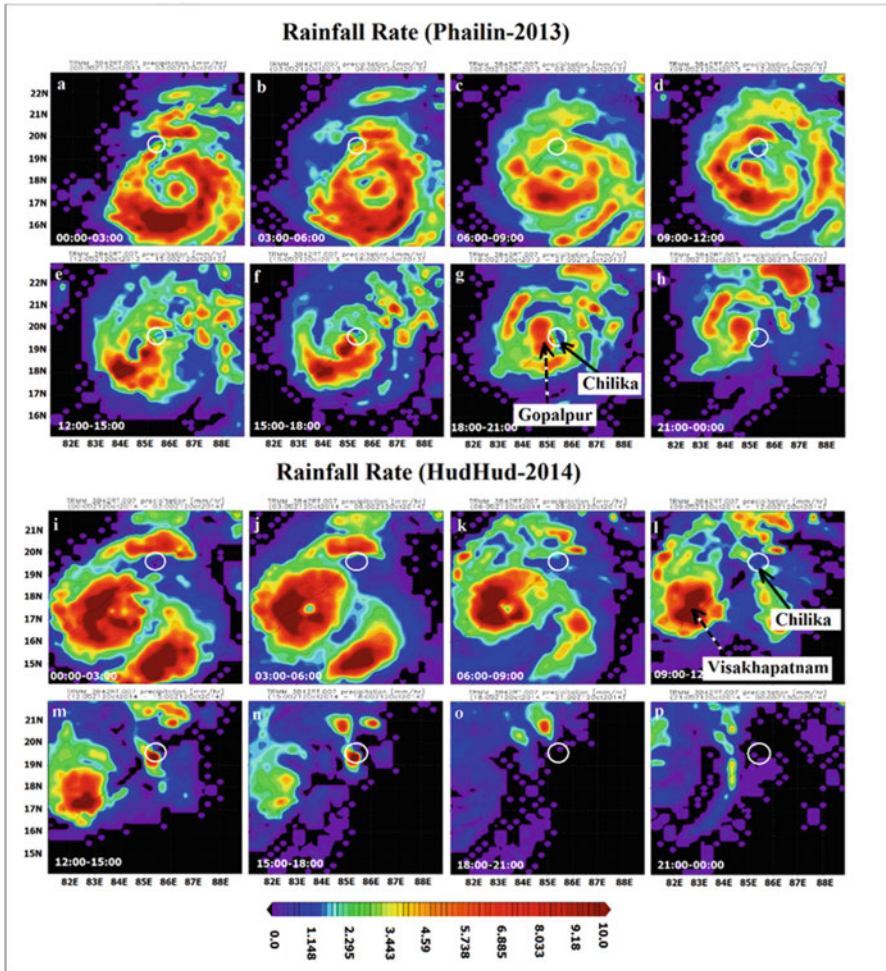


Fig. 8.8 Precipitation map produced by Giovanni web based application tool using TRMM 3-hourly product for 24 h on the landfall day of *Phailin* (October 12, 2013) and *Hudhud* (October 12, 2014). Chilika Lagoon is indicated by solid arrows with open circle and the landfall points are indicated by dashed arrows (g and l)

4379.45 $\text{g/m}^2\text{-h}^{-1}$; WC: highest up to 683.25 $\text{g/m}^2\text{-h}^{-1}$) due to high precipitation (NC: highest up to 17076.28 $\text{g/m}^2\text{-h}^{-1}$; WC: highest up to 9198.02 $\text{g/m}^2\text{-h}^{-1}$) in contrast to relatively lower surface runoff on the landfall day of *Hudhud* (NC: highest up to 532.48 $\text{g/m}^2\text{-h}^{-1}$; WC: highest up to 253.41 $\text{g/m}^2\text{-h}^{-1}$) due to comparatively less precipitation (NC: highest up to 5279.74 $\text{g/m}^2\text{-h}^{-1}$; WC: highest up to 4852.47 $\text{g/m}^2\text{-h}^{-1}$) and passage of *Hudhud* from sector with lesser tributaries and more vegetated areas.

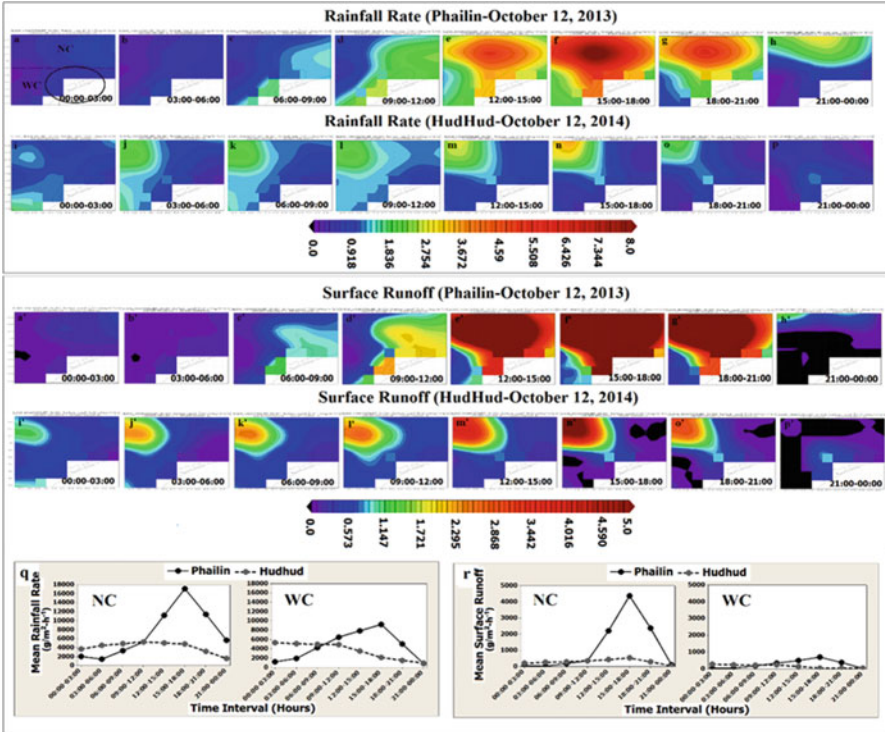


Fig. 8.9 Rainfall rate (a–p) and surface runoff (a’–p’) map produced by Giovanni web based application tool using GLDAS 3-hourly products for the 24 h on the landfall day of *Phailin* (October 12, 2013) and *Hudhud* (October 12, 2014) near the catchment area. The two catchments northern (NC: 19.9° S – 20.4° N; 84.6° W – 85.8° E) and western (WC: 19.4° W – 19.9° N; 84.6° W – 85.2° E) used in comparative analysis are demarcated by dashed lines and Chilika Lagoon is marked with open circle (a). Catchment-wise comparison of rainfall rate (q) and surface runoff at every 3 h (r)

The surface runoff transects in both cases indicated that the maximum contribution was from northern and north-western zone (together considered as NC), where the lagoon receives highest surface runoff due to the heavy discharge from rivers and distributaries, compared to WC (Fig. 8.9; also, refer to Fig. 8.7a, b). The northern catchment includes agricultural land, bare ground, and urban areas, which primarily contributed to the surface runoff compared to the western watershed which is mainly comprised of forested land. Also, the downward sloping topography and major tributaries of Mahanadi River of NC supports higher surface runoff and the Khallikote forest present in the WC of the lagoon limits the surface runoff to a large extent. Previous studies also documented relatively higher runoff in agricultural and urbanized watershed which elevated nutrients and suspended sediments to nearby water bodies (Jordan et al. 2003; Mallin and Corbett 2006; Wetz and Yoskowitz 2013). The surface runoff transects revealed a significant increase in magnitude (~1 order of magnitude increase) after 12:00 p.m. on the landfall day of

Phailin and it persisted for continuous 9 h (Fig. 8.9e'-g', r). In contrast, there was no such order difference observed during VSCS *Hudhud* in the magnitude of surface runoff (Fig. 8.9i-p, r). The primary reason behind difference in runoff associated with the two cyclones was the speed of passage which is characterized as a determining factor associated with the magnitude of impact of such VSCSs in previous literatures (Mallin and Corbett 2006; Srichandan et al. 2015). For example, Mallin and Corbett (2006) observed that the fast moving hurricane *Andrew* resulted in low erosion compared to hurricane *Dennis* which lingered for several days over the watershed near North Carolina and resulted in enhanced runoff. The speed of passage for *Hudhud* was much faster (~9–12 h) compared to *Phailin* (>24 h) over the watershed of Chilika, which caused the difference in rainfall amount and duration. This difference led to the highly variable surface runoff from the watershed of the lagoon. The above results were primarily from the landfall day of both VSCSs. To quantify the variability of these parameters under normal environmental conditions, both pre-and post-cyclone data corresponding to entire month of October 2013 and 2014 were analysed (Fig. 8.10). Also, an additional variable, near surface wind speed was incorporated in further analysis.

Figure 8.10 shows the variability in mean surface wind speed, mean rainfall rate (surface precipitation), and mean surface runoff for overall catchment corresponding to the entire month before-during-after the cyclones (October 2013 and 2014). The gradual increase in surface wind speed started on October 9, 2013 (9.82 km/h) and reached to peak level on the landfall day of *Phailin* (October 12, 2013: 53.72 km/h) (Fig. 8.10a). Similar increase in surface wind speed started on October 7, 2014 (7.18 km/h) and continued to increase till the landfall day of *Hudhud* when it reached at its peak level (October 12, 2014: 35.55 km/h). The wind speed magnitude on the landfall day was 51% higher for *Phailin* compared to *Hudhud* (Table 8.4). Unlike wind speed, the rainfall rate and surface runoff increased at an exponential rate on the landfall day and decreased at the same rate after the passage of the cyclones. High sustained wind and runoff may have triggered the re-suspension of bottom sediments which increased the turbidity in the lagoon drastically on the landfall day of *Phailin*. An earlier study based on field measurement of turbidity in the lagoon has shown that before *Phailin* the turbidity of the lagoon was 32.8 NTU which increased to 60.4 NTU after *Phailin* (Srichandan et al. 2015). In contrast, comparatively lower mean surface runoff ($243.97 \text{ g/m}^2\text{-h}^{-1}$) due to lower mean surface precipitation ($3809.33 \text{ g/m}^2\text{-h}^{-1}$) and lower wind speed on the landfall day of *Hudhud* was not able to increase the turbidity of the lagoon to *Phailin* level (Table 8.4) (Fig. 8.7f). The magnitude and spatial distribution of turbidity in the lagoon on the aftermath of these cyclones are primarily determined by wind speed and runoff. While massive runoff resulting from heavy rainfall brings substantial amount of sediments to the lagoon and can be considered as the primary driver of turbidity, high wind speed triggers sediment re-suspension and is a secondary source of turbidity. Wind speed which plays the major role in sediment re-suspension during cyclonic events (Chen et al. 2009; Wetz and Yoskowitz 2013) was significantly higher during *Phailin* compared to *Hudhud* which may have triggered additional turbidity in the lagoon. It is important to break down and analyse the physical and meteorological factors

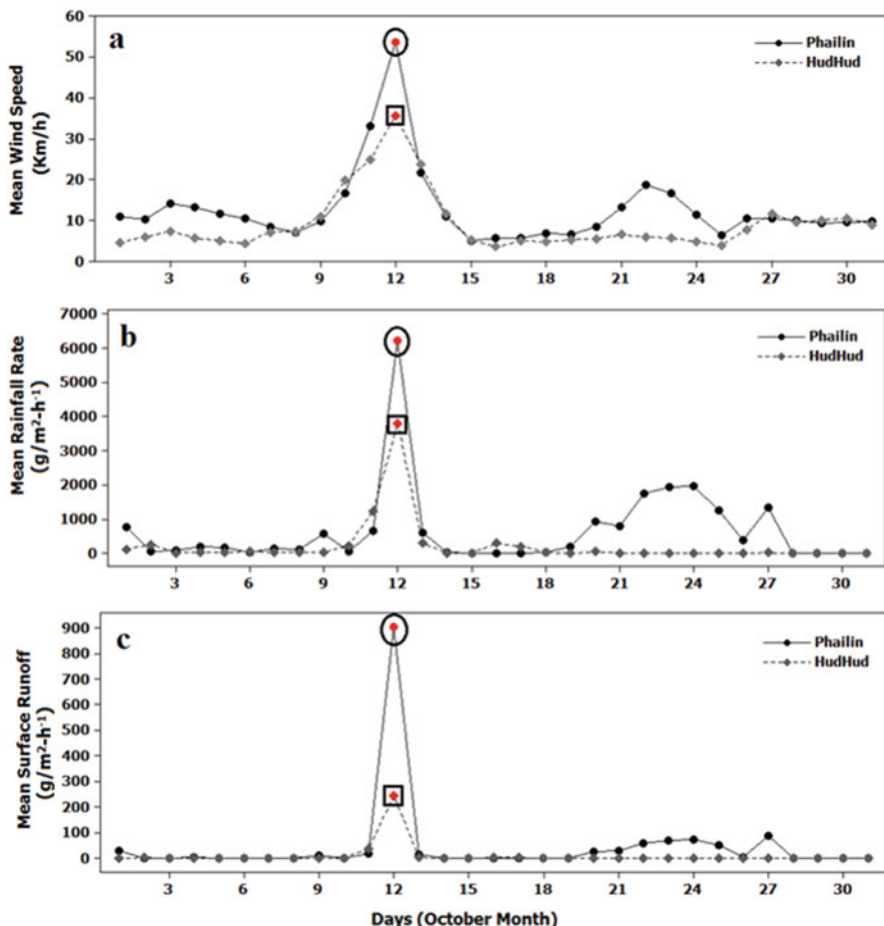


Fig. 8.10 Variation in meteorological parameters: mean surface wind speed and mean rainfall rate (a–b) and physical parameter: mean surface runoff (c) corresponding to overall catchment (19.4° N – 20.4° N and 84.6° E – 85.8° E) surrounding the Chilika Lagoon for October (X-axis: Days of October 2013 and 2014; Y-axis: mean surface runoff, mean rainfall rate and mean surface wind speed). The open circles and boxes indicated the unprecedented level of magnitude on the landfall day for both VSCSs, *Phailin* (October 12, 2013) and *Hudhud* (October 12, 2014) respectively

because they are strongly linked to the turbidity which is ultimately linked to the likelihood of an algal bloom after the passage of a cyclone. Wind induced bottom sediment re-suspension is also dependent on sediment types and size (Havens et al. 2011). The sediment size varies in different sectors of Chilika Lagoon such as fine sediments (silt and clay) in offshore (NS and CS) due to major river extracts, and coarser sediment (sand) in nearshore (SS and OC) because of exchange of sea water through the mouth (Raman et al. 2007; Ansari et al. 2015). Therefore, NS and CS which are dominated by fine sediment experienced higher degree of re-suspension

Table 8.4 Comparison between physical and meteorological parameters for the entire October and landfall day for both cyclones corresponding to overall catchment (19.4° N – 20.4° N and 84.6° E – 85.8° E) surrounding the Chilika Lagoon

Parameters	October – entire month			Landfall day		
	<i>Phailin</i> (October, 2013)	<i>Hudhud</i> (October, 2014)	%Higher (<i>Phailin</i>)	<i>Phailin</i> October 12, 2013	<i>Hudhud</i> October 12, 2014	%Higher (<i>Phailin</i>)
Mean surface wind speed (km/h)	12.79	9.33	+37.08%	53.72	35.55	+51.11%
Mean rainfall rate (g/m ² -h ⁻¹)	658.12	222.03	+196.41%	6235.21	3809.33	+63.68%
Mean surface runoff (g/m ² -h ⁻¹)	44.71	9.6	+365.72%	904.16	243.97	+270.61%

leading to high turbidity compared to SS. Havens et al. (2011) reported similar phenomena that fine sediments in central part of Lake Okeechobee were more susceptible to re-suspension after increases in wind velocity and caused more limitation of light compared to near shore coarse sediment.

Impact of anniversary VSCSs on the lagoon was further investigated with the MODIS derived TSS and Chl-*a* concentration. The mean TSS concentration was found to be significantly higher in NS (*Phailin*: 131.36 mg/L; *Hudhud*: 75.13 mg/L) and CS (*Phailin*: 35.32 mg/L; *Hudhud*: 13.53 mg/L) during October 2013 (*Phailin* month) compared to October 2014 (*Hudhud* month) (Fig. 8.11, Table 8.5). Difference in precipitation, surface runoff, and wind speed all combinedly created this differential impact. The mean TSS in SS was observed to be very similar in magnitude between October 2013 (16.24 mg/L) and 2014 (15.33 mg/L) and lowest among all sectors (Fig. 8.11, Table 8.5). This is because SS was the least affected section due to low surface runoff from western side of the lagoon. In contrast, the mean Chl-*a* concentration was found to be relatively higher for the month of *Hudhud* compared to *Phailin* in all the sectors (*Phailin*: NS: 4.21 µg/L, CS: 11.36 µg/L, SS: 21.94 µg/L; *Hudhud*: NS: 6.93 µg/L, CS: 18.44 µg/L, SS: 24.61 µg/L) of the lagoon (Fig. 8.11, Table 8.5). Massive increase in turbidity in the water column after *Phailin* reduced the transparency level and limited the availability of light (Srichandan et al. 2015). The limited light availability affected the Chl-*a* concentration, an indicator of primary productivity, which reduced significantly post-*Phailin* in all the sectors of the lagoon. Srichandan et al. (2015) also reported a significant decrease in Chl-*a* concentration immediately after *Phailin* in Chilika Lagoon and no sign of phytoplankton bloom after the passage. Previous studies also reported reduced phytoplankton biomass after the passage of cyclone due to significant light attenuation in water column (Paerl et al. 1998; Mallin et al. 2002; Mallin and Corbett 2006; Srichandan et al. 2015).

One important difference found from Fig. 8.11b, d is the lag effect of cyclones on phytoplankton growth in different sectors of the lagoon. It took more than a week

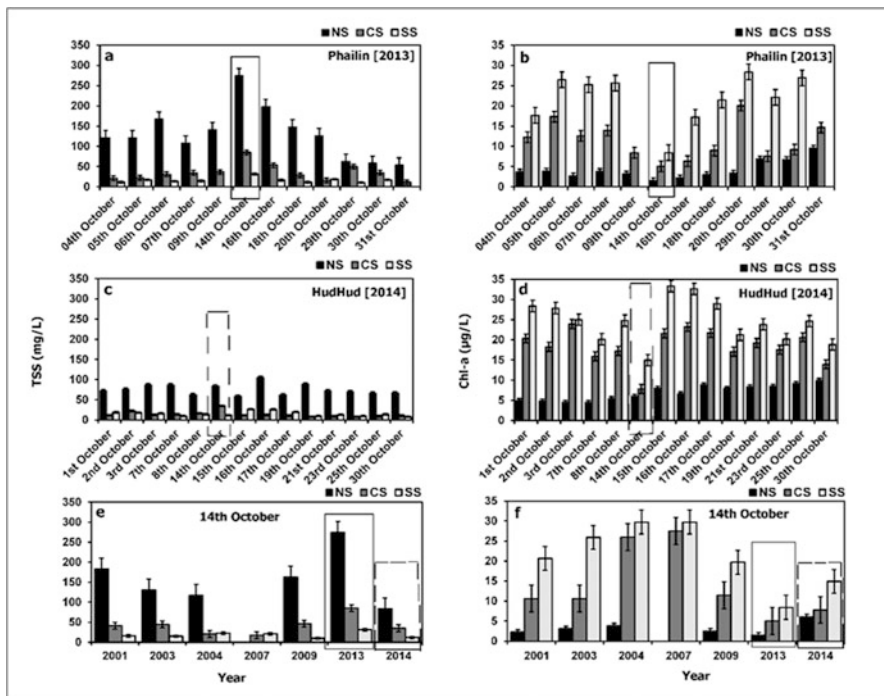


Fig. 8.11 Variations in mean TSS and mean Chl-*a* concentration across the three sectors of the lagoon (NS, CS, SS). The bars inside the solid box and dashed box represent the readings 2 days after the landfall of VSCSs *Phailin* and *Hudhud*. TSS and Chl-*a* data was not included from SS of the lagoon on October 09, 2013 and from NS of the lagoon on October 14, 2007 due to cloud cover

Table 8.5 Sector-wise statistics of TSS and Chl-*a* concentration measured during October (2013 and 2014) for both VSCSs

γ	Sector	Cyclone month	Minimum	Maximum	Range	Mean	Standard deviation
Mean TSS (mg/L)	NS	<i>Phailin</i> :	53.22	274.05	220.83	131.36	± 62.84
		<i>Hudhud</i> :	58.05	104.48	46.43	75.13	± 13.02
	CS	<i>Phailin</i> :	11.61	84.99	73.38	35.32	± 19.94
		<i>Hudhud</i> :	7.67	35.04	27.37	13.53	± 7.26
	SS	<i>Phailin</i> :	10.55	31.30	20.75	16.24	± 5.97
		<i>Hudhud</i> :	7.82	26.99	19.17	15.33	± 5.98
Mean Chl- <i>a</i> ($\mu\text{g/L}$)	NS	<i>Phailin</i> :	1.48	9.61	8.13	4.21	± 2.35
		<i>Hudhud</i> :	4.46	9.91	5.45	6.93	± 1.78
	CS	<i>Phailin</i> :	5.05	20.04	14.99	11.36	± 4.56
		<i>Hudhud</i> :	7.81	23.91	16.10	18.44	± 4.16
	SS	<i>Phailin</i> :	8.42	28.35	19.93	21.94	± 6.10
		<i>Hudhud</i> :	14.93	33.31	18.38	24.61	± 5.27

Data were extracted from 27 locations (9 from each sector (NS, CS, and SS)) and averaged out for each sector to obtain the mean TSS and mean Chl-*a* concentration as presented below

after the passage of *Phailin* for the mean Chl-*a* concentration to recover to pre-*Phailin* level comparing the sector-wise values between October 7th and 20th, 2013 (October 7, 2013 – NS: 3.8 µg/L; CS: 13.89 µg/L; SS: 25.62 µg/L and October 20, 2013 – NS: 3.41 µg/L; CS: 20.04 µg/L; SS: 28.35 µg/L). However, only 2 days after the passage of *Hudhud*, i.e., on October 15, 2014 the mean Chl-*a* concentration (NS: 8.01 µg/L; CS: 21.59 µg/L; SS: 33.31 µg/L) crossed the pre-*Hudhud* level (October 7, 2014 – NS: 4.46 µg/L; CS: 15.9 µg/L; SS: 20.13 µg/L). This could be related to the combined effect of light availability and nutrient enrichment in the water column, just suitable enough to favor the phytoplankton growth. For example, field data collected from the lagoon suggested that there was about tenfold increase in nitrate concentration in Chilika lagoon after *Hudhud* compared to pre-*Hudhud* month. The turbidity of the lagoon in September 2014 was 138 NTU which decreased to 95.4 NTU in October 2014 after *Hudhud*. The reduced turbidity (increased transparency) along with other favourable meteorological, physical, and hydrological factors (calm wind, low precipitation, discharge, runoff, and low flushing rate) created suitable environment for phytoplankton growth as evidenced with the fact that average phytoplankton density before *Hudhud* (September 2014) was 2200 cells/mL which increased to 6216 cells/mL after *Hudhud* (October 2014).

Further, spatial maps corresponding to TSS and Chl-*a* concentration derived from MOD09GQ products followed similar pattern corresponding to true color MODIS images which verified the implication of biophysical models (Fig. 8.12). The maps were divided into two segments (red dash line); pre-VSCSs (pre- *Phailin* and pre-*Hudhud*) period (left) and post-VSCSs period (right) (Fig. 8.12). Visual analysis of the true color MODIS images clearly showed the highly turbid NS in all images (Fig. 8.12). The spatio-temporal pattern of TSS and Chl-*a* concentration pre-VSCSs period showed the usual gradients as discussed in the previous sections. There was consistent cloud cover over the lagoon starting from October 9 (2013 and 2014) which limited the availability of cloud free MODIS images close to the landfall date for both VSCSs. However, just 2-days after *Phailin*, on October 14, 2013, MODIS true color image (inside the circle: Fig. 8.12) showed a remarkable increase in turbidity throughout the lagoon and similar pattern was obtained when the TSS model was implemented on MODIS data. On the contrary, Chl-*a* map post-*Phailin* showed a substantial decrease throughout the lagoon on October 14, 2013 (inside the circle: Fig. 8.12) which could be due to the high TSS concentration that did not allow algal growth as discussed in earlier section. However, this result was in contradiction to many previous literatures that reported enhanced phytoplankton biomass after the passage of cyclones or a anthropogenic massive runoff (Angles et al. 2015; Sarangi et al. 2014; Huang et al. 2011; Mishra and Mishra 2010; Paerl et al. 2001, 2006; Mallin et al. 2006; Peierls et al. 2003). For example, similar increase was reported in recent studies by Sarangi et al. (2014) and Lotliker et al. (2014) in north-west region of BOB post-*Phailin*. Both studies correlated sea surface temperature (SST) with Chl-*a* concentration and concluded that enhanced nutrient supply due to mixing of water column and stratification of layer created a favourable condition for phytoplankton growth. However, Chilika is a shallow lagoon (depth range: 0.5–3.0 m) where stratification is not a major problem and there has been no evidence of

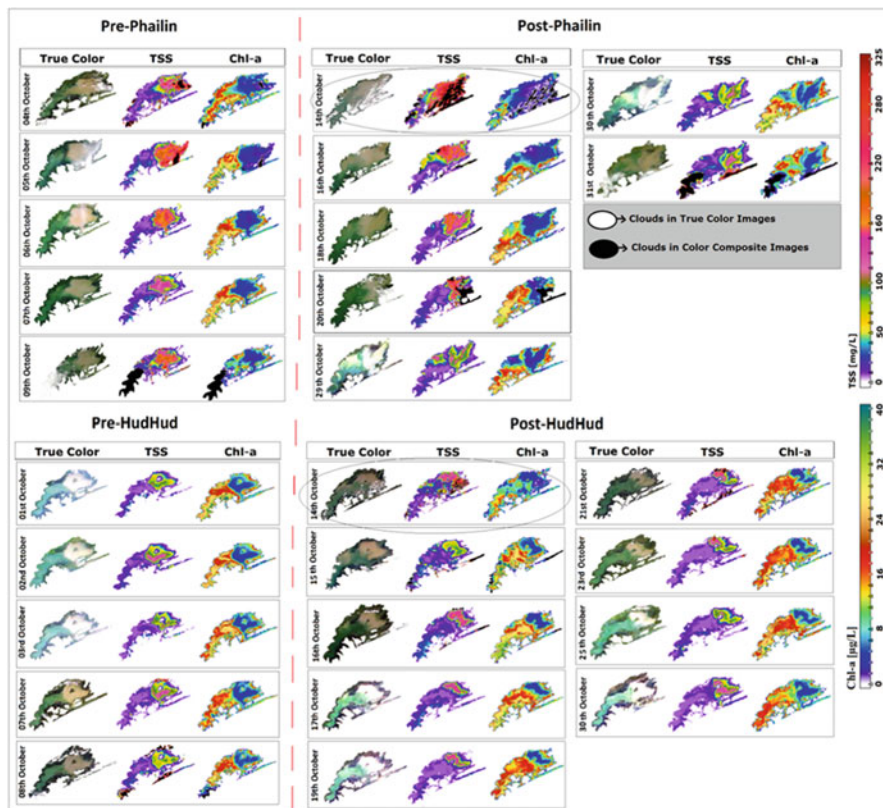


Fig. 8.12 Spatial and temporal variation of TSS and Chl-*a* concentration in Chilika Lagoon pre-during-post VSCSs (*Phailin*: October 2013 and *Hudhud*: October 2014) using MODIS true color images. The images inside the circles show the immediate aftermath of the VSCSs. Gaps observed in the dates are due to the unavailability of cloud free MODIS products

stratification in the lagoon based on 12 years of data (2000–2011) analyzed by CDA (Kumar and Pattnaik 2012). On the other hand, mixing of water column due to high wind action during cyclonic events may circulate large amount of nutrients from bottom of the lagoon to upper layers. These nutrients help proliferate phytoplankton growth if environmental conditions are supportive such as sufficient light, calm wind, and low flushing rate. These favourable environmental conditions were not available post-*Phailin* which restricted the phytoplankton growth. Additionally, Bacillariophyta and Dinophyta are the dominant phytoplankton species in the lagoon which require highly saline and transparent waters to grow but their growth was restricted post-*Phailin* because of very high freshwater discharge and storm water runoff which reduced salinity and increased turbidity to a great extent in the lagoon (Srichandan et al. 2015). Other studies have also concluded that re-suspension of the sediments increases the nutrient availability which triggers algal growth (Zhu et al. 2014; Sarangi et al. 2014). However, that was not the case after *Phailin*. Turbidity in

the lagoon started reducing as the days progressed after the passage of *Phailin* because the sediment started settling down to the bottom and consequently, Chl-*a* concentration recovered back to pre-cyclone level after a week of the passage, but a phytoplankton bloom was not observed (Fig. 8.12).

On the other hand, post-*Hudhud* TSS maps did not show a significant change in TSS and a gradual increase in Chl-*a* concentration was observed throughout the lagoon (Fig. 8.12). There were several factors contributed for this differential impact post-*Hudhud*. For example, *Hudhud* made landfall relatively at farther distance from Chilika, stayed for shorter duration, and moved away from the lagoon after its landfall. The combination of landfall location, duration, and trajectory during *Hudhud* resulted in lower precipitation and surface runoff in the watershed of the lagoon. As a result, any sector of the lagoon did not experience an increase in TSS to the level of post-*Phailin*. However, through satellite imagery a phytoplankton bloom was observed with Chl-*a* concentration increasing three-times after the passage of *Hudhud*. Previous studies also suggested that when there is sufficient light available in the water column followed by tropical cyclone, stimulation of phytoplankton becomes more rapid (Miller et al. 2006; Wetz and Paerl 2008; Wetz and Yoskowitz 2013). Chilika Lagoon experienced a sudden increase in Chl-*a* just after 2-days of landfall of *Hudhud* and the upward trend continued for few more days. A gradual spread in the spatial coverage of increased Chl-*a* concentration from SS towards NS was clearly visible in post-*Hudhud* MODIS derived Chl-*a* maps (Fig. 8.12). This type of sudden increase in Chl-*a* is common in previous studies (Peierls et al. 2003; Paerl et al. 2010; Huang et al. 2011; Sarangi et al. 2014; Lotliker et al. 2014; Baliarsingh et al. 2015). For example, Huang et al. (2011) reported sudden increase in mean Chl-*a* from 5.3 to 14.7 $\mu\text{g/L}$ in Pensacola Bay, Florida just after a day of passage of Hurricane *Ivan*. In another study, Baliarsingh et al. (2015) reported a significant increase in Chl-*a* just after 3-days of landfall of *Hudhud* in north-western BOB from 1.58–2.28 mg/m^3 to 2.57–6.62 mg/m^3 . They attributed this increase to nutrient entrainment from river influx due to the VSCS.

In the above discussion, a combination of several factors was attributed to the differential impact of two cyclones on the water quality of the lagoon. However, isolating a single factor primarily responsible for the differential impact would not be useful because each individual factor has its own importance and often correlated with other factors. For example, distance from landfall location cannot be isolated from the trajectory and speed of the cyclone. Past studies have reported that even if a cyclone makes landfall close to study area but passes very quickly, then it would not bring as much amount of rainfall and runoff compared to a slow moving cyclone which stayed for a longer duration (Mallin and Corbett 2006). Similarly surface runoff cannot be isolated from precipitation, nutrient pulsing cannot be isolated from mixing of water column. The same principle is applicable to the phytoplankton growth in a lagoon which requires a combination of several factors favourable for primary production. Srichandan et al. (2015) suggested that several other factors such as nutrient, turbidity, water residence time, and flushing rate are equally important for phytoplankton biomass production along with geographic-geomorphologic-bathymetric setting of an estuary. For instance, high flushing rate

in combination with high fresh water discharge limited the phytoplankton growth in Neuse River Estuary post-Hurricane *Fran* (Paerl et al. 1998). Similarly, rapid flushing for several weeks was reported post-*Phailin* in Chilika Lagoon that slowed the rate of phytoplankton growth (Srichandan et al. 2015). Flushing rate was comparatively less rapid post-*Hudhud* as the flood intensities in the distributaries were much lower compared to *Phailin*. Another factor suggested by Wetz and Yoskowitz (2013) was calm wind after the passage of cyclone supports the stratification and light condition for phytoplankton growth. The wind speed was stable after the passage of *Hudhud* but wind speed was dynamic post-*Phailin* that might have slowed down the phytoplankton growth in the lagoon. Therefore, lower rainfall, lower surface runoff, less turbidity, low flushing rate, and stable wind, all favored the phytoplankton bloom post-*Hudhud*. The same factors but at a different magnitude prevented a phytoplankton bloom post-*Phailin*. The above results and discussions validated the proposed hypothesis that the likelihood of a phytoplankton bloom or significant increase in phytoplankton biomass after a cyclone is dependent on the physical, meteorological, and geomorphological characteristics of the VSCS and the lagoon.

8.4 Summary and Conclusion

This study showed that MODIS daily surface reflectance products (MOD09GQ) and MODIS 8-day composite products (MOD09Q1) are well suited for monitoring the biophysical parameters (TSS and Chl-*a*) concentration in Chilika Lagoon. MOD09GQ product can be used for short-term monitoring purpose, while MOD09Q1 can be used for long-term assessment. The result of quantitative analysis for 14 years (2001–2014) using MODIS 8-day composites (MOD09Q1) data indicated that the seasonal variability of TSS is dominant in all the three sectors of the Chilika Lagoon compared to inter-annual variability. The main reason for large variations in the northern sector is the shallow depth and intrusion of large sediment discharge from Mahanadi River from the northern side, which is the largest fresh water distributary for Chilika Lagoon. Similar findings such as high turbidity in NS followed CS and SS (Mohanty and Pal 2001), significant seasonal variability in water surface area and water quality parameters (Pal and Mohanty 2002) have also been reported in the past using field based measurements. However, this study analyzed additional contribution of physical and meteorological factors from different catchment area of the lagoon in increasing the TSS level. It was also found that monthly mean TSS (2001–2014) for NS and CS is strongly correlated with total precipitation and surface runoff compared to SS. However, TSS in southern sector was highly correlated with wind stress compared to the other two sectors. Overall, results indicated that different factors have different level of impact on the TSS variability across the three sectors of the lagoon.

Further, a case study showed the day-to-day applicability of the biophysical models for tracking the effect of natural hazards and other physical and

geomorphological changes on the water quality of the lagoon. This case study primarily dealt with questions such as why some cyclones trigger phytoplankton blooms in estuaries and lagoons and some don't? and what factors control the likelihood of a bloom after the passage of a cyclonic storm? A comprehensive comparative analysis of several factors was performed to isolate the causes of the differential impact of anniversary VSCSs, *Phailin* and *Hudhud*, on the water quality of Chilika Lagoon. The anniversary VSCSs allowed the verification of a theoretical concept widely discussed in previous literatures that characteristics of a cyclone such as close landfall location, high wind intensity, longer duration of stay, trajectories along the watershed of study area would support high precipitation and surface runoff which may lead to increased turbidity and a phytoplankton bloom in nearby water bodies such as estuaries and lagoons (Wetz and Yoskowitz 2013; Mallin and Corbrett 2006; Paerl et al. 2001). *Phailin's* impact on Chilika Lagoon and its watershed resulted in unprecedented levels of precipitation and runoff before-during-after the landfall, which shattered the typical sectorial turbidity gradient. Exponential increase in turbidity because of a combination of run-off and wind driven re-suspension of fine sediments resulted in strong attenuation of light in water column post-*Phailin*. Limited light condition coupled with enhanced flushing rate due to flooded river and increased fresh water discharge reduced the Chl-*a* concentration after the passage of *Phailin*. In contrast, relatively farther landfall location, trajectory away from the lagoon, relatively lower wind intensity and short duration of stay of VSCS *Hudhud*, led to lesser precipitation and surface runoff compared to *Phailin*. Consequently, lagoon did not experience a drastic increase in turbidity and light attenuation. Sufficient light availability, stable wind, reduced flushing all favored the phytoplankton growth after passage of *Hudhud* and as a result, Chl-*a* concentration increased almost threefold in all the sectors of the lagoon.

The frequency of tropical cyclones is expected to increase under the global climate change scenario which makes satellite based high spatial and temporal assessment very useful compared to field sampling program which are limited in spatial and temporal domain (Srichandan et al. 2015). Satellite data coupled with model derived products may become very useful in near future for the assessment of cyclone induced impact and predicting phytoplankton bloom prone areas. The approach used in this study can be applied to other cyclone-prone coastal areas. Coupling of satellite based observation with modelling output from systems such as Giovanni can improve monitoring program implemented in numerous coastal estuaries and lagoons. Susceptible watershed areas that contribute in high surface runoff can be isolated and management plan can be implemented like creating buffer zone or plantation to minimize the surface erosion rate which is a major factor in deteriorating water quality of any lake. Also, long-term monitoring ability of satellite based model will facilitate researchers and regulators to assess the changes in estuarine and lake system and associated watershed on a broader scale. The ability to predict these changes on estuarine and coastal environments might become an essential part of designing and implementing the management and restoration effort for a lake, estuary, or coastal region in future. Overall, high frequency monitoring of physical, biophysical, and meteorological parameters using satellite data can help in

tracking several environmental phenomena in the lagoon such as siltation, effectiveness of dredging activities, areas with high probability of algal blooms, impact of high TSS on seagrass habitats, and the overall water clarity and productivity of the lagoon.

Acknowledgements AK, the lead author, thanks NIT Rourkela for financial assistance in the form of institute fellowship. This work is a part of Master's thesis submitted by AK to NIT Rourkela. QuikScat data used in this study are produced by Remote Sensing Systems and sponsored by the NASA Ocean Vector Winds Science Team. The authors wish to thank the Goddard Space Flight Center (GSFC), NASA and MODIS support team for providing region specific MODIS satellite data products and Giovanni datasets.

References

- Acker J, Leptoukh G (2007) Online analysis enhances use of NASA earth science data. *EOS Trans Am Geophys Union* 88(2):14–17
- Acker J, Soebiyanto R, Kiang R, Kempler S (2014) Use of the NASA Giovanni data system for geospatial public health research: example of weather-influenza connection. *ISPRS Int J Geo Inf* 3:1372–1386
- Angles S, Jordi A, Campbell L (2015) Responses of the coastal phytoplankton community to tropical cyclones revealed by high-frequency imaging flow cytometry. *Limnol Oceanogr* 60:1562–1576
- Ansari KGMT, Pattnaik AK, Rastogi G, Bhadury P (2015) An inventory of free-living marine nematodes from Asia's largest coastal lagoon, Chilika, India. *Wetl Ecol Manag* 23(2):881–890. <http://dx.doi.org/10.1007/s11273-015-9426-2>
- Astuti I, Mishra DR, Mishra S, Schaeffer B (2018) A hybrid approach for deriving inherent optical properties in oligotrophic estuaries. *Cont Shelf Res* 166:92–107
- Baliarsingh SK, Parida C, Lotliker AA, Srichandan S, Sahu KC, Kumar TS (2015) Biological implications of cyclone Hudhud in the coastal waters of northwestern Bay of Bengal. *Curr Sci* 109(7):1243–1245
- Binding CE, Bowers DG, Mitchelson-Jacob EG (2005) Estimating suspended sediment concentration from ocean colour measurements in moderately turbid waters; the impact of variable particle scattering properties. *Remote Sens Environ* 94:373–383
- Bramha S, Panda UC, Bhatta K, Sahu BK (2008) Spatial variation in hydrological characteristics of Chilika-A coastal lagoon of India. *Indian J Sci Technol* 1(4):1–7
- Cao F, Mishra DR, Schalles J, Miller W (2018) Evaluating ultraviolet (UV) based photochemistry in optically complex coastal waters using the Hyperspectral Imager for the Coastal Ocean (HICO). *Estuar Coast Shelf Sci* 215:199–206
- CDA (Chilika Development Authority) (2008) The atlas of Chilika. Chilika Development Authority, Bhubaneswar
- Chaichitehrani N, D'Sa EJ, Osburn CL, Bianchi TS, Schaeffer BA (2013) Chromophoric dissolved organic matter and dissolved organic carbon from SeaWiFS, MODIS and MERIS sensors: case study for the northern Gulf of Mexico. *Remote Sens* 5:1439–1464
- Chen Z, Hu C, Muller-Karger F (2007) Monitoring turbidity in Tampa Bay using MODIS/Aqua 250-m imagery. *Remote Sens Environ* 109:207–220
- Chen S, Huang W, Wang H, Li D (2009) Remote sensing assessment of sediment re-suspension during Hurricane Frances in Apalachicola Bay, USA. *Remote Sens Environ* 113:2670–2681
- Cui L, Qiu Y, Fei T, Liu Y, Wu G (2013) Using remotely sensed suspended sediment concentration variation to improve management of Poyang Lake, China. *Lake Reservoir Manage* 29:47–60

- Dekker AG, Peters SWM, Vos RJ (2001) Comparison of remote sensing data, model results and in situ data for total suspended matter (TSM) in the Southern Frisian Lakes. *Sci Total Environ* 268:197–214
- Dekker AG, Vos RJ, Peters SW (2002) Analytical algorithms for lake water TSM estimation for retrospective analyses of TM and SPOT sensor data. *Int J Remote Sens* 23(1):15–35
- Dogliotti AI, Ruddick KG, Nechad B, Doxaran D, Knaeps E (2015) A single algorithm to retrieve turbidity from remotely-sensed data in all coastal and estuarine waters. *Remote Sens Environ* 156:157–168
- Doxaran D, Froidefond JM, Castaing P, Babin M (2009) Dynamics of the turbidity maximum zone in a macrotidal estuary (the Gironde, France): observation from field and MODIS satellite data. *Estuar Coast Shelf Sci* 81:321–332
- El-Alem A, Chokmani K, Laurion I, El-Adlouni SE (2012) Comparative analysis of four models to estimate chlorophyll-a concentration in case-2 waters using MODERate Resolution Imaging Spectroradiometer (MODIS) imagery. *Remote Sens* 4:2373–2400
- Fang H, Hrubiak PL, Kato H, Rodell M, Teng WL, Vollmer BE (2008) Global Land Data Assimilation System (GLDAS) products from NASA Hydrology Data and Information Services Center (HDISC). ASPRS 2008 annual conference Portland, Oregon April 28 – May 2, 2008. <http://www.asprs.org/a/publications/proceedings/portland08/0020.pdf>
- Fox RC, Rowntree KM (2013) Extreme weather events in the Sneeuwberg, Karoo, South Africa: a case study of the floods of 9 and 12 February 2011. *Hydrol Earth Syst Sci Discuss* 10:10809–10844
- Gitelson AA, Gritz Y, Merzlyak MN (2003) Relationships between leaf chlorophyll content and spectral reflectance and algorithms for non-destructive chlorophyll assessment in higher plant leaves. *J Plant Physiol* 160:271–282
- GoO (2013) Memorandum on the very severe Cyclone Phailin and the subsequent flood 12–15 October 2013. The Revenue and Disaster Management Department Government of Odisha. <http://www.osdma.org/userfiles/file/MEMORANDUMPhailin.pdf>. Accessed 10 Oct 2014
- Gupta M (2013) Chromaticity analysis of the Chilika lagoon for total suspended sediment estimation using RESOURCESAT-1 AWiFS data- a case study. *J Great Lakes Res* 39:696–700
- Havens KE, Beaver JR, Casamatta DA, East TL, James RT, McCormick P, Philips EJ, Rodusky AJ (2011) Hurricane effects on the planktonic food web of a large subtropical lake. *J Plankton Res* 33:1081–1094
- Hu C, Chen Z, Clayton T, Swarnzenski P, Brock J, Muller-Karger F (2004) Assessment of estuarine water quality indicators using MODIS medium-resolution bands: initial results from Tampa Bay, Florida. *Remote Sens Environ* 93:423–441
- Huang W, Mukherjee D, Chen S (2011) Assessment of Hurricane Ivan impact on chlorophyll-a in Pensacola Bay by MODIS 250 m remote sensing. *Mar Pollut Bull* 62(3):490–498
- IFRC (1999) Cyclone: Orissa, India Information Bulletin No. 1. International Federation of Red Cross (IFRC) and Red Crescent Societies. <http://www.ifrc.org/docs/appeals/rpts99/in005.pdf>. Accessed 10 Oct 2014
- IMD (2013) Very severe cyclonic storm, PHAILIN over the Bay of Bengal (08–14 October 2013): a report. <http://www.imd.gov.in/section/nhac/dynamic/phailin.pdf>
- IMD (2014) Very severe cyclonic storm, HUDHUD over the Bay of Bengal (07–14 October 2014): a report. <http://www.rsmcnewdelhi.imd.gov.in/images/pdf/publications/preliminary-report/hud.pdf>
- Jayaraman G, Rao AD, Dube A, Mohanty PK (2005) Numerical simulation of circulation and salinity structure in Chilika lagoon. *J Coast Res* 22:195–211
- Jordan TE, Whigham DF, Hofmockel KH, Pittek MA (2003) Wetlands and aquatic processes: nutrient and sediment removal by a restored wetland receiving agricultural runoff. *J Environ Qual* 32:1534–1547
- Kahru M, Mitchell BG, Diaz A, Miura M (2004) Modis detects a devastating algal bloom in Paracas Bay, Peru. *Eos* 85(45):465–472

- Katlane R, Dupouy C, Zargouni F (2012) Chlorophyll and turbidity concentrations as an index of water quality of the Gulf of Gabes from MODIS in 2009. *Teledetection* 11(1):265–273
- Kumar R, Pattnaik AK (2012) Chilika – an integrated management planning framework for conservation and wise use. Wetlands International – South Asia, New Delhi, India and Chilika Development Authority, Bhubaneswar, India
- Kumar A, Equeenuddin S, Mishra DR, Acharya BC (2016) Remote monitoring of sediment dynamics in a coastal lagoon: long-term spatio-temporal variability of suspended sediment in Chilika. *Estuar Coast Shelf Sci* 170:155–172
- Lee Z, Carder KL, Chen RF, Peacock TG (2001) Properties of the water column and bottom derived from Airborne Visible Infrared Imaging Spectrometer (AVIRIS) data. *J Geophys Res Oceans* 106(C6):11639–11651
- Lotliker AA, Srinivasakumar T, Reddem VS, Nayak S (2014) Cyclone Phailin enhanced the productivity following its passage: evidence from satellite data. *Curr Sci* 106(3):360–361
- Madrinan MJM, Hamdan ZAM, Rickman DL, Muller-Karger F (2010) Using the surface reflectance MODIS Terra product to estimate turbidity in Tampa Bay, Florida. *Remote Sens* 2:2713–2728
- Mallin MA, Corbrett CA (2006) How hurricane attributes determine the extent of environmental effects: multiple hurricanes and different coastal systems. *Estuar Coasts* 29:1046–1061
- Mallin MA, Posey MH, McIver MR, Parsons DC, Ensign SH, Alphin TD (2002) Impacts and recovery from multiple hurricanes in a Piedmont-coastal plain river system. *Bioscience* 52:999–1010
- Mallin MA, Johnson VL, Ensign SH, MacPherson TA (2006) Factors contributing to hypoxia in rivers, lakes and streams. *Limnol Oceanogr* 51(2):690–701
- Miller RL, McKee BA (2004) Using MODIS 250 m imagery to map concentration of total suspended matter in coastal waters. *Remote Sens Environ* 93:259–266
- Miller WD, Harding LW, Adolf JE (2006) Hurricane Isabel generated an unusual fall bloom in Chesapeake Bay. *Geophys Res Lett* 33:L06612. <http://dx.doi.org/10.1029/2005GL025658>
- Miller RL, Liu CC, Buonassissi CJ, Wu AM (2011) A multi-sensor approach to examining the distribution of Total Suspended Matter (TSM) in the Albemarle-Pamlico estuarine system, NC, USA. *Remote Sens* 3:962–974
- Mishra DR, Gould R Jr (2016) Preface: remote sensing in coastal environments. *Remote Sens* 8(8):665
- Mishra DR, Mishra S (2010) Plume and bloom: effect of Mississippi river diversion on the water quality of Lake Pontchartrain. *Geocarto Int* 25(7):555–568
- Mishra S, Mishra DR (2012) Normalized difference chlorophyll index: a novel model for remote estimation of chlorophyll-*a* concentration in turbid productive waters. *Remote Sens Environ* 117:394–406
- Mishra SP, Panigrahi DR (2014) Storm impact on south Odisha coast, India. *Int J Adv Res Sci Eng* 3(11). ISSN: 2319-8354 (E)
- Mishra S, Mishra DR, Lee Z, Tucker C (2013) Quantifying cyanobacterial phycocyanin concentration in turbid productive waters: a quasi-analytical approach. *Remote Sens Environ* 133:141–151
- Mishra S, Mishra DR, Lee Z (2014a) Bio-optical inversion in highly turbid and cyanobacteria dominated waters. *IEEE Trans Geosci Remote Sens* 52:375–388
- Mishra DR, Schaeffer BA, Keith D (2014b) Performance evaluation of normalized difference chlorophyll index in northern Gulf of Mexico estuaries using the hyperspectral imager for the coastal ocean. *GISci Remote Sens* 51(2):175–198
- Mishra DR, Ogashawara I, Gitelson AA (2017) Bio-optical modeling and remote sensing of inland waters, 1st edn. Elsevier, Waltham, p 332. ISBN: 9780128046449
- Mohanty PK, Pal SR (2001) IRS data utilisation for estimation of turbidity level in Chilika lagoon, east coast of India. In: Proceedings of 22nd Asian conference on remote sensing, 5–9 November 2001, Singapore

- Mohanty PK, Panda BUS (2009) Circulation and mixing processes in Chilika lagoon. *Indian J Mar Sci* 38(2):205–214
- Nayak BK, Acharya BC, Panda UC, Nayak BB, Acharya SK (2004) Variation of water quality in Chilika Lake, Orissa. *Indian J Mar Sci* 33(2):164–169
- Ogashawara I, Mishra DR, Gitelson AA (2017) Remote sensing of inland waters: background and current state-of-the-art. In: Mishra DR, Ogashawara I, Gitelson AA (eds) *Bio-optical modeling and remote sensing of inland waters*, 1st edn. Elsevier, Waltham, p 332. ISBN: 9780128046449
- Paerl HW, Pinckney JL, Fear JM, Peierls BL (1998) Ecosystem responses to internal and watershed organic matter loading: consequences for hypoxia in the eutrophying Neuse River Estuary, North Carolina, USA. *Mar Ecol Prog Ser* 166:17–25
- Paerl HW, Bales JD, Ausley LW, Buzzelli CP, Crowder LB, Eby LA, Fear JM, Go M, Peierls BL, Richardson TL, Ramus JS (2001) Ecosystem impacts of 3 sequential hurricanes (Dennis, Floyd and Irene) on the US's largest lagoonal estuary, Pamlico Sound, NC. *Proc Natl Acad Sci U S A* 98(10):5655–5660
- Paerl HW, Valdes LM, Peierls BL, Adolf JE, Harding LW (2006) Anthropogenic and climatic influences on the eutrophication of large estuarine ecosystems. *Limnol Oceanogr* 51:448–462
- Paerl HW, Rossignol KL, Hall SN, Peierls BL, Wetz MS (2010) Phytoplankton community indicators of short- and long term ecological change in the anthropogenically and climatically impacted Neuse River Estuary, North Carolina, USA. *Estuar Coasts* 33:485–497
- Page B, Kumar A, Mishra DR (2018) A novel cross-satellite based assessment of the spatio-temporal development of a cyanobacterial harmful algal bloom. *Int J Appl Earth Obs Geoinf* 66:69–81
- Pal SR, Mohanty PK (2002) Use of IRS-1B data for change detection in water quality and vegetation of Chilika Lagoon, east coast of India. *Int J Remote Sens* 23(6):1027–1042
- Panda US, Mohanty PK (2008) Monitoring and modelling of Chilika environment using remote sensing data. In: *Proceedings of Tail 2007: the 12th world lake conference*, 28 October-2 November 2007, Jaipur, India, pp 617–638
- Panigrahi S, Winker J, Panigrahy RC, Satpathy KK, Acharya BC (2009) Variability of nutrients and phytoplankton biomass in a shallow brackish water ecosystem (Chilika Lagoon, India). *Limnology* 10:73–85
- Patnaik SS (1998) Estimation of sediment flow into the Chilika Lake. Abstract volume, workshop on sustainable development of Chilika Lake, Orissa (Bhubaneswar, India: Chilika Development Authority), pp 31–32
- Peierls B, Christian R, Paerl H (2003) Water quality and phytoplankton as indicators of hurricane impacts on a large estuarine ecosystem. *Estuaries* 26:1329–1343
- Petus C, Chust G, Gohin F, Doxaran D, Froidefond JM, Sagarminaga Y (2010) Estimating turbidity and total suspended matter in the Adour River Plume (South Bay of Biscay) using MODIS 250-m imagery. *Cont Shelf Res* 30:379–392
- Prasad AK, Singh RP (2010) Chlorophyll, calcite and suspended sediment concentrations in the Bay of Bengal and the Arabian Sea at the river mouths. *Adv Space Res* 45:61–69
- Raman AV, Kalavati C, Prabhakara Rao Y (2007) Modelling Chilka Lake: an ecosystem approach. Final report (2004–07) submitted to Ministry of Earth Sciences ICMAM Directorate Chennai. <http://www.icmam.gov.in/CHIL.PDF>
- Rao DP, Subramanian SK, Sudarsana R (1986) Geomorphic analysis of Chilika Lake and adjoining area using remotely sensed data, Photonirvachak. *J Indian Soc Remote Sens* 14:53–60
- Ritchie JC, Zimba PV, Everitt JH (2003) Remote sensing technique to assess water quality. *Photogramm Eng Remote Sens* 69(6):695–704
- Rodell M, Houser PR (2004) Updating a land surface model with MODIS derived snow cover. *J Hydrometeorol* 5(6):1064–1075
- Sarangi RK, Mishra MK, Chauhan P (2014) Remote sensing observations on impact of Phailin cyclone on phytoplankton distribution in northern Bay of Bengal. *IEEE J Sel Top Appl Earth Observ Remote Sens* 8(2):539–549

- Siddiqi SZ, Rama Rao KV (1995) Fauna of Chilika Lake: limnology, zoological survey of India. *Wetl Ecosyst Ser* 1:11–136
- Srichandan S, Kim JY, Kumar A, Mishra DR, Bhadury P, Muduli PR, Pattnaik AK, Rastogi G (2015) Interannual and cyclone-driven variability in phytoplankton communities of a tropical coastal lagoon. *Mar Pollut Bull* 101(1):39–52
- Sudhakar S, Pal DK (1993) Water quality assessment of the Lake Chilka. *Int J Remote Sens* 14:2575–2579
- UNEP (2013) Cyclone Phailin in India: early warning and timely actions saved lives. http://www.unep.org/pdf/UNEP_GEAS_NOV_2013.pdf
- Vermote EF, El saleoql N, Justice CO, Kaufman YJ, Privette JL, Remer L, Roger JC, Tanre D (1997) Atmospheric correction of visible to middle-infrared EOS-MODIS data over land surfaces: background, operational algorithm and validation. *J Geophys Res* 102:17131–17141
- Wang G, Lee Z, Mishra DR, Ma R (2016) Retrieving absorption coefficients of multiple phytoplankton pigments from hyperspectral remote sensing reflectance measured over cyanobacteria bloom waters. *Limnol Oceanogr Methods* 14(7):432–447
- Wetz MS, Paerl HW (2008) Estuarine phytoplankton responses to hurricanes and tropical storms with different characteristics (trajectory, rainfall, winds). *Estuar Coasts* 31:419–429
- Wetz MS, Yoskowitz DW (2013) An ‘extreme’ future for estuaries? Effects of extreme climatic events on estuarine water quality and ecology. *Mar Pollut Bull* 69(2013):7–18
- Zhang Y, Lin S, Liu J, Qian X, Ge Y (2010) Time-series MODIS image-based retrieval and distribution analysis of total suspended matter concentrations in Lake Taihu (China). *Int J Environ Res Public Health* 7(9):3545–3560
- Zhang Y, Lin S, Qian X, Wang Q, Qian Y, Liu J, Ge Y (2011) Temporal and spatial variability of chlorophyll a concentration in Lake Taihu using MODIS time-series data. *Hydrobiologia* 661:235–250
- Zhao HH, Chen Q, Walker ND, Zheng QA, MacIntyre HL (2011) A study of sediment transport in a shallow estuary using MODIS imagery and particle tracking simulation. *Int J Remote Sens* 32(21):6653–6671
- Zhu M, Paerl HW, Zhu G, Wu T, Li W, Shi K, Zhao L, Zhang Y, Qin B, Caruso AM (2014) The role of tropical cyclones in stimulating cyanobacterial blooms in hypertrophic Lake Taihu, China. *Harmful Algae* 39:310–321